ปริมาณรังสีที่อวัยวะได้รับในการตรวจเอกซเรย์คอมพิวเตอร์สมอง ทรวงอก และช่องท้อง จากเครื่องเอกซเรย์คอมพิวเตอร์ชนิดหลายตัวรับภาพ

นางรติรัตน์ เผือกพ่วง

วิทยานิพนธ์นี้เป็นส่วนหนึ่งของการศึกษาตามหลักสูตรปริญญาวิทยาศาสตรมหาบัณฑิต
สาขาวิชาฉายาเวชศาสตร์ ภาควิชารังสีวิทยา
คณะแพทยศาสตร์ จุฬาลงกรณ์มหาวิทยาลัย
ปีการศึกษา 2553

ORGAN DOSES IN BRAIN AND BODY MULTIDETECTOR COMPUTED TOMOGRAPHY EXAMINATION

Mrs. Ratirat Puekpuang

A Thesis Submitted in Partial Fulfillment of the Requirements
for the Degree of Master of Science Program in Medical Imaging
Department of Radiology
Faculty of Medicine
Chulalongkorn University
Academic Year 2010

Thesis Title	ORGAN DOSES IN BRAIN AND BODY MULTIDETECTOR COMPUTED TOMOGRAPHY EXAMINATION
By	Mrs. Ratirat Puekpuang
Field of Study	Medical Imaging
Thesis Advisor	Associate Professor Sivalee Suriyapee, M.Eng.

Accepted by the Faculty of Medicine, Chulalongkorn University in Partial Fulfillment of the Requirements for the Master's Degree

.....Dean of the Faculty of Medicine
(Professor Adisorn Patradul, M.D.)

THESIS COMMITTEE

.....Chairman
(Associate Professor Kiat Arjhansiri, M.D.)

.....Thesis Advisor
(Associate Professor Sivalee Suriyapee, M.Eng.)

.....Examiner
(Assistant Professor Panruethai Trinavarat, M.D.)

.....External Examiner
(Professor Franco Milano, Ph.D.)

รติรัตน์ เผือกพ่วง: ปริมาณรังสีที่อวัยวะได้รับในการตรวจเอกซเรย์คอมพิวเตอร์สมอง ทรวงอกและช่องท้อง จากเครื่องเอกซเรย์คอมพิวเตอร์ชนิดหลายตัวรับภาพ. (ORGAN DOSES IN BRAIN AND BODY MULTIDETECTOR COMPUTED TOMOGRAPHY EXAMINATION) อ.ที่ปรึกษาวิทยานิพนธ์หลัก: รศ. ศิวลี สุริยาปี, 75 หน้า.

การตรวจด้วยเอกซเรย์คอมพิวเตอร์ (ซีที) เป็นสิ่งจำเป็นในการวินิจฉัยโรคด้วยรังสี มีการใช้มัลติดีเทคเตอร์ซีที (เอ็มดีซีที) กันอย่างแพร่หลาย เนื่องมาจากข้อดีทางเทคโนโลยี การประเมินความเสี่ยงจากรังสีและประโยชน์จากการตรวจวินิจฉัยด้วยรังสี จึงเป็นสิ่งสำคัญ ปริมาณรังสีที่อวัยวะได้รับและปริมาณรังสียังผลคือปริมาณสำคัญที่ใช้ในการประเมินค่าความเสี่ยงจากรังสี แต่เป็นการยากที่ทำการวัดปริมาณรังสีในผู้ป่วย แต่ละบุคคล ดังนั้นจุดประสงค์ของการศึกษานี้ เพื่อคำนวณปริมาณรังสีที่อวัยวะและปริมาณรังสียังผลได้รับ ในการตรวจตามโปรโตคอลของส่วนสมอง ทรวงอก และช่องท้อง ด้วยวิธีมอนติคาร์โล โดยการใช้โปรแกรมคำนวณปริมาณรังสีในผู้ป่วยอิมแพคท์ซีทีเวอร์ชั่น 1.0 ด้วยการเก็บข้อมูลการตรวจ จากผู้ป่วยผู้ใหญ่จำนวน 60 คน ในแต่ละการตรวจทั้งเพศชายและเพศหญิง จากเครื่องเอกซเรย์ 64 สไลซ์ ของบริษัทจีอี รุ่นวีซีที ความแม่นยำของการคำนวนปริมาณรังสีตรวจสอบด้วย การวัดแบบเทอร์โมลูมิเนสเซนต์ (ทีแอลดี) ในหุ่นจำลอง แอลเดอร์สันแรนโด

การตรวจสอบความแม่นยำของปริมาณรังสียังผล ที่ประมาณค่าจากการวัดด้วยทีแอลดี เปรียบเทียบกับการจำลอง ตามโปรโตคอลการตรวจทรวงอกและช่องท้องได้ผลสอดคล้องกันดีใน 4.3 เปอร์เซ็นต์ แต่ในการตรวจสมอง มีความแตกต่างถึง 20.5 เปอร์เซ็นต์ สำหรับผู้ป่วยค่าความยาวเฉลี่ยของการสแกนผู้ป่วยในการตรวจสมองเท่ากับ 13.4 $\pm$ 0.65 เซนติเมตร ในการตรวจส่วนทรวงอกเท่ากับ 34.3 $\pm$ 4.99 เซนติเมตร และในการตรวจส่วนช่องท้องทั้งหมดเท่ากับ 41.4 $\pm$ 3.13 เซนติเมตร ปริมาณรังสีที่อวัยวะได้รับในบริเวณที่ตรวจสมอง คือ 37 มิลลิเกรย์ในสมอง และ 43 มิลลิเกรย์ ในเลนส์ตา ในการตรวจส่วนทรวงอกปริมาณรังสีตั้งแต่ 12 ถึง 19 มิลลิเกรย์ พบที่ปอด เต้านม หลอดอาหาร ต่อมหมวกไต ไทมัส และหัวใจ ในการตรวจช่องท้องทั้งหมด ปริมาณรังสีตั้งแต่ 16 ถึง 22 มิลลิเกรย์ พบที่ ลำไส้ใหญ่ กระเพาะอาหาร กระเพาะปัสสาวะ ตับ ต่อมหมวกไต ลำไส้เล็ก ไต ตับอ่อน ม้าม รังไข่ มดลูกและต่อมลูกหมาก ค่าปริมาณรังสียังผลเฉลี่ย 1.6 $\pm$ 0.07 มิลลิซีเวิร์ต, 7.2 $\pm$ 1.03 มิลลิซีเวิร์ต และ 9.7 $\pm$ 0.46 มิลลิซีเวิร์ต สำหรับการตรวจส่วนสมอง ส่วนทรวงอกและส่วนช่องท้องทั้งหมดตามลำดับ ปริมาณรังสียังผลต่ำกว่าข้อแนะนำของ ไอซีอาร์พี ประมาณ 3 ถึง 25 เปอร์เซ็นต์ ค่าความเสี่ยงการตายจากมะเร็งโดยผลของรังสีประมาณ 1, 4 และ 5 ต่อประชากร 10,000 คน ในการตรวจส่วนสมอง ส่วนทรวงอกและส่วนท้องทั้งหมดตามลำดับ โดยสรุป ค่าความยาวในการสแกน คือ หนึ่งในตัวแปร ที่ทำให้ปริมาณรังสีที่อวัยวะและปริมาณรังสียังผลสูงขึ้น จำนวนรอบการสแกนของการตรวจ คือปัจจัยที่เพิ่มปริมาณรังสีจากการตรวจเอกซเรย์คอมพิวเตอร์ การคำนวณค่าปริมาณรังสีที่อวัยวะและปริมาณรังสียังผล เป็นหนึ่งในปัจจัยที่กำหนดเป็นตัวชี้วัดสำหรับรังสีแพทย์และแพทย์ ในการสรุปการใช้ความถี่ในการสแกนและความยาวในการสแกนที่เหมาะสม

ภาควิชา.....รังสีวิทยา.....ลายมือชื่อนิสิต.....

สาขาวิชา.....ฉายาเวชศาสตร์.....ลายมือชื่อ อ. ที่ปรึกษาวิทยานิพนธ์หลัก.....

ปีการศึกษา.....2553.....

#5274801130: MAJOR MEDICAL IMAGING
KEYWORDS: ORGAN DOSES / MONTE CARLO SIMULATION / THERMOLUMINESCENT DOSIMETRY

RATIRAT PUEKPUANG: ORGAN DOSES IN BRAIN AND BODY MULTIDETECTOR COMPUTED TOMOGRAPHY EXAMINATION. THESIS ADVISOR: ASSOC.PROF.SIVALEE SURIYAPEE, 75 pp.

Computed tomography (CT) examinations are an essential part of the diagnostic procedures in radiology. Multidetector CT (MDCT) is becoming more and more widespread due to advances in technology. Evaluation of radiation risk and benefit is important in all radiation diagnostic procedures. The organ and effective doses are the important quantities to assess radiation risk, but an individual CT patient dose is not possible to be measured exactly. The objective of this study is to determine organ doses and effective doses in brain, chest and abdomen protocols by Monte Carlo method using ImPACT CT Patient Dosimetry Calculator version 1.0. The patient data was collected from 64 slices GE VCT scanner of 60 cases in each examination in adult male and female. The accuracy of dose calculation was verified with thermoluminescent dosimeters (TLDs) measurement in Alderson Rando phantom.

The verification of the effective dose estimated from TLD dose measurements for chest and abdomen protocol showed a good agreement within 4.3% with the Monte Carlo simulation while the brain protocol showed the difference of 20.5%. For patient data collection, the average patient scan lengths were 13.4±0.65 cm for brain, 34.3±4.99 cm for chest and 41.4±3.13 cm for whole abdomen examinations. The high organ doses in irradiated field showed 37 mGy in brain and 43 mGy in eye lenses for brain examination, the dose ranged from 12 to 19 mGy occurred in lung, breast, esophagus, adrenal gland, thymus and heart for chest examination and the dose ranged from 16 to 22 mGy occurred in colon, stomach, bladder, liver, adrenal gland, small intestine, kidney, pancreas, spleen, ovaries, uterus and prostate for whole abdomen examination. The average effective doses were 1.6±0.07 mSv, 7.2±1.03 mSv and 9.7±0.46 mSv for brain, chest and whole abdomen examination, respectively. The effective doses were about 3 to 25% lower than the ICRP recommendation. The estimated fatal cancer risks were about 1, 4 and 5 cases for 10,000 populations in brain, chest and whole abdomen examinations, respectively. The scan length is one of the variable factors that make the high organ and effective doses in CT examination. The more series of examination is another factor to increase the CT doses. Estimated organ and effective doses provide an approximate indicator of potential detriment from radiation for radiologists and physicians to use as the parameters in evaluating the frequency of scan and suitable scan length.

Department: ……Radiology……...Student's Signature…….

Field of Study: …….Medical imaging……Advisor's Signature…….

Academic Year: ……...2010……

ACKNOWLEDGEMENTS

I would like to express gratitude and deepest appreciation to Associate Professor Sivalee Suriyapee, M.Eng., Division of Radiation Oncology, Department of Radiology, Faculty of Medicine, Chulalongkorn University, my advisor, for her guidance, helpful suggestion, supervision, constructive comments and polishing of the thesis writing to improve the readability and English expression.

I would like to extremely greatly Associate Professor Anchali krisanachinda, Ph.D., Division of Nuclear Medicine, Department of Radiology, Faculty of Medicine, Chulalongkorn University, my teacher for her invaluable advices, constructive comments.

I would like to extremely thank Mr. Taweap Sanghangthum, M.Sc., my co-advisor, Mr.Sornjarod Oonsiri, M.Sc., Miss Puntiwa Insang, M.Sc., the medical physic staffs at Division of Radiation Oncology, King Chulalongkorn Memorial Hospital, for their helpful suggestion and encouragement and providing the required equipments to perform, improve English language and format in this research.

I would like to deeply thank Mrs. Siripan Kalayanarooj, MD. Head of Department of Radiology, Miss Sunee Lumlertdacha medical staff in Department of Radiology, Rajavithi Hospital to their instruction of using the machine, facilitated in providing the required instrument, useful advices and encouragement.

I would like to deeply thank Associate Professor Kiat Arjhansiri, MD., Head of Division of Diagnostic Radiology, and Assistant Professor Panruethai Trinavarat, M.D, in, Division of Diagnostic Radiology, Department of Radiology, Faculty of Medicine, Chulalongkorn University for advice and comments in the research.

I would like to deeply thank Professor Franco Milano, Ph.D. from University of Florence Italy, who external examiner of this thesis defense for his helpful concentrate of recommendation, constructive comments and teaching of knowledge in Medical Imaging.

I would like to thank Mrs. Petcharleeya Suwanpradit, M.Sc., Department of Radiology , King Chulalongkorn Memorial Hospital and all of the staff at Division of Radiation Oncology, King Chulalongkorn Memorial Hospital, for kindness advice, support of instruments experimental for this research. I would like to thank medical staff in Department of Radiology, Rajavithi Hospital, who facilitated of using the machine for their helps in this research.

I would like to thank Mrs. Weeranuch Kitsukjit for her provide suggestion for the improvement. I am thankful for all teachers, lecturers and staff in the Master of Science Program in Medical Imaging, Faculty of Medicine, and Chulalongkorn University for their unlimited teaching of knowledge in Medical Imaging.

Finally, I am extremely grateful to my family for their financial support, invaluable encouragement, entirely and understanding during the entire course of study.

CONTENTS

Page

CHAPTER III RESEARCH METHODOLOGY

LIST OF TABLES

LIST OF FIGURES

LIST OF ABBREVIATIONS

ABBREVIATION	TERMS
AEC	Automatic exposure control
$^{\circ}c$	Degree Celsius
cm	centimeter
^{60}Co	Cobolt-60
^{137}Cs	Cesium-137
CT	Computed tomography
CTDI	Computed tomography Dose Index
$CTDI_w$	Weight Computed tomography Dose Index
$CTDI_{vol}$	Volume Computed tomography Dose Index
DLP	Dose length product
ECC	Element Correction Coefficient
ED	Effective dose
FOV	Field of view
g/cm^3	gram per cubic centimeter
ICRP	International Commission on Radiological Protection
ICRU	International Commission on Radiation Units and Measurement
ImPACT	The Imaging Performance Assessment of CT Scanners
kV	kilovoltage
LiF	Lithium Fluoride
mA	milliampare
mAs	milliampare - second
mGy	milliGray
mm	millimeter
mmAl	millimeter-aluminum
mSv	milliSivert
MDCT	Multidetector computed tomography
MSCT	Multislice computed tomography
nC	nano-Culomb
NRPB	The National Radiological Protection Board
PMMA	Polymethyl methacrylate acrylic
PMT	Photomultiplier tube

ABBREVIATION	TERMS
QC	Quality Control
RCF	Radiation Correction Factor
Sv	Sievert
TL	Thermoluminescent
TLDs	Thermoluminescent dosimetors

CHAPTER I

INTRODUCTION

1.1 Background and rationale

Computed Tomography (CT) is one of the most important methods of radiological diagnosis. It displays cross-sectional images of the body, which can show smaller contrast differences than conventional X-ray images. The development of slip ring technology allowed for a continuously rotating gantry for spiral CT. The Multidetector Computed Tomography (MDCT) was introduced in the early 1990s which the scanner developed from third generation CT geometry in which the arc of detectors and the x-ray tube rotate together and the evolution of CT from single slice spiral CT through 4 slices, to 16 slices, up to 64 slices, and nowadays the newly technology have been grown up to 640 slices. The principle basis of its advantages is the ability to scan large anatomic range, make faster scan, and reduce examination times. The growth of MDCT associated with the large number of images per examination offers many clinical benefits. The MDCT is an imaging tool that is widely used for examination in most of the organs, it is easy to use for radiologist and physician, and these reasons are the cause of increasing exposure for populations rapidly. It constitutes the largest contribution to the radiation exposure of the population from diagnostic medical sources.

The hazard of ionizing radiation must be considered, CT scans contribute the higher radiation dose compared to conventional x-ray because the systems designed for the large volume scanning. The various CT scanning protocols are used for different examinations and some protocol may contribute the high dose. Moreover, the numbers of scan in each examination are more than one because routine technique is analyzed by radiologist and is repeated when physician followed up. The increase in the number of MDCT has been paralleled by increasing the organ and effective doses. Those are the important quantities using for estimate risk of radiation-induced cancers, which focused on dose to individual organs and tissues. The CT patient dose is not possible to be measured for the exact organ dose and effective dose and the various kinds of human tissue and organs have different sensitivities for radiation. The individual dose is also affected by characteristics of patients. To estimate radiation dose to organs, Monte Carlo radiation transport codes have been developed to simulate CT examinations.

The objective of this study is to determine organ doses and effective doses in brain, chest and whole abdomen examinations in 64 slices MDCT for 60 patients in each group of examination by the Imaging Performance Assessment of CT Scanners (ImPACT) Monte Carlo calculation method. The accuracy of dose calculation is verified with thermoluminescent dosimeters (TLDs) measurement in Alderson Rando phantom.

1.2 **Research objectives**

To determine brain and body average organ doses in Multi-Detector Computed Tomography scan.

CHAPTER II

REVIEW OF RELATED LITERATURE

2.1 Theory

2.1.1 Principle of MDCT [1]

Computed Tomography (CT) involves the data collection, image reconstruction and image display (image manipulation, storage, recording and communication) of cross-sectional anatomy. MDCT scanners are based on the third generation CT system design. The basic components of a CT scanner are an x-ray tube and arc of detectors, mounted on a gantry with a circle aperture they are shown in Fig.2.1. The patient lies on an integral couch, the X-ray tube and detectors rotate continuously, while the absorption of X-rays changes following body changes. Image data can be acquired in sequential mode or in helical mode. Along the patient long axis there are many rows of these arcs of detectors, giving rise to the term multislice CT (MSCT) or multidetector CT are also commonly used terms.

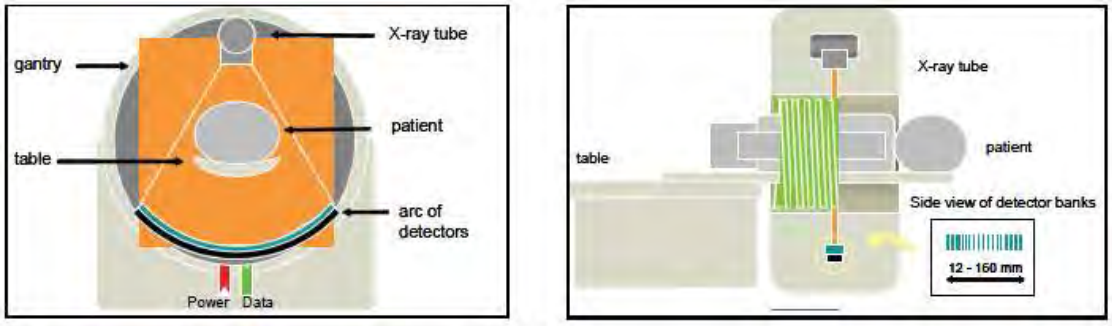

a) b)

Fig.2.1 Schematic diagram of the CT scanner.
a) 'End view' of the CT scanner b) 'Side view' in helical acquisition mode

2.1.2 MDCT system design

By 2004, 64-slice scanners were announced. MDCT scanners have progressively been increased the number of detectors and reduced scan acquisition times. Detector array designs were to lengthen the arrays in the z-direction and provide all submillimeter detector elements: 64 x 0.625 mm (total z-axis length of 40 mm) for General Electric Healthcare (GE) and Phillips models, however, different vender has different detector design.

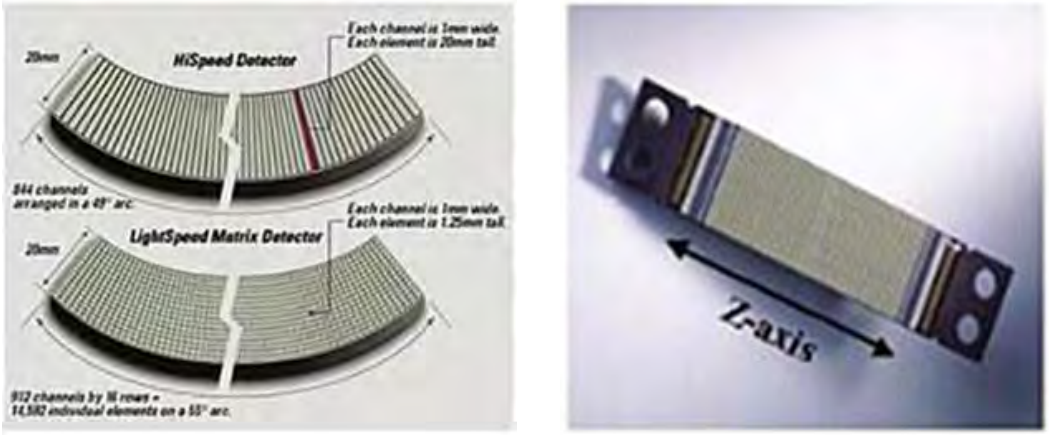

a) b)

Fig.2.2 Diagrams of various 64-slice detector designs (in z-direction).
a) GE LightSpeed detector b) Aquillion 16 detector

Most designs lengthen arrays and provide all submillimeter elements. GE Medical Systems is shown in Fig.2.2a and Toshiba Medical System is shown in Fig.2.2b.

2.1.3 Quantification of dose in CT [2]

2.1.3.1 Computed Tomography Dose Index (CTDI)

The Computed Tomography Dose Index (CTDI) is the fundamental CT dose descriptor. It was defined as the integral of the dose profile, D (z), from a single axial scan along a line perpendicular to the tomographic plane (z-axis) divided by the nominal slice thickness (T):

$$CTDI = \frac{1}{T}\int_{-\infty}^{+\infty} D(z) \cdot dz \qquad (2.1)$$

For the case of MSCT scanners, where N slices of thickness T are acquired during a single axial scan, the following equation is used

$$CTDI_{100} = \frac{1}{NT}\int_{-50}^{+50} D(z) \cdot dz \qquad (2.2)$$

$CTDI_{100}$ is measured by pencil type ionization chamber with an active length of 100 mm, both in free air and within two cylindrical polymethylacrylate phantoms of 16 cm and 32 cm diameter, simulating the head and body of a patient, respectively. $CTDI_{100}$ measured with the ionization chamber positioned in free air at the centre of rotation is referred to as $CTDI_{air}$. $CTDI_c$ and $CTDI_p$ are defined respectively as the $CTDI_{100}$ values measured with the ionization chamber within the centre and four positions (12 o'clock, 3 o'clock, 6 o'clock and 9 o'clock) in the periphery (1 cm from the surface) of the head and body phantoms, which are centrally positioned within the gantry. All CTDI quantities are given in units of mGy.

2.1.3.2 Weighted CTDI

The weighted CTDI (CTDIw) is used for approximating the average dose over a single slice and is defined by the following equation, separately for the head and the body phantoms.

$$CTDI_w = \frac{1}{3} CTDI_{100,c} + \frac{2}{3} CTDI_{100,p} \quad (2.3)$$

Where the average of the four roughly CTDIp values measured in the periphery of the phantom is used.

2.1.3.3 Volume Weighted CTDI

The volume weighted CTDI (CTDIvol) is used to account for helical scanning and is defined by the following equation

$$CTDI_{vol} = \frac{CTDI_w}{Pitch\ factor} = CTDI_w \cdot \frac{NT}{I} \quad (2.4)$$

Where NT is the total nominal collimation width and I is the table travel per rotation during a helical scan (pitch factor = I/NT).

2.1.3.4 Dose length product

Dose length product (DLP) is used to calculate the dose for a series of scans or a complete examination and is defined by the following equation

$$DLP = \sum_{i=N}^{N} CTDI_{vol} \times L \quad (2.5)$$

Where i represents each of the individual scans of the examination that covers a length Li of patient anatomy. DLP is given in units of mGy cm.

2.1.3.5 Equivalent Dose

The equivalent dose (H_T) is a measure of the radiation dose to tissue where an attempt has been made to allow for the different relative biological effects of different types of ionizing radiation. Equivalent dose is calculated by multiplying the absorbed dose to the organ or tissue with the radiation-weighting factor. This factor is selected for the type and energy of the radiation incident on the body, or in the case of sources within the body, emitted by the source. The value of radiation weighting factor is 1 for x-rays, gamma rays and beta particles, but higher for protons, neutrons, and alpha particles. Equivalent dose has units of Sieverts.

$$H_T = \sum_T W_R \, A_T \quad (2.6)$$

Where A_T is the organ dose, H_T is the organ equivalent dose, and W_R is radiation weighting factor.

2.1.3.6 Effective Dose

Effective dose (E) is a quantity that has been introduced to quantify the biological detriment resulting from a partial body irradiation, enabling the calculation of radiological risk. Its calculation is based on the application of tissue-weighting factors (W_T) on the equivalent doses (H_T) absorbed by the various radiosensitive organs of the human body. The unit for the effective dose is Sv. That is:

$$E = \sum W_T \cdot H_T \tag{2.7}$$

For this study the organ and tissue weighting factors recommended by the International Commission on Radiological Protection (ICRP) publication 103 [3] are used as shown in Table 2.1.

Table 2.1 Organ and tissue weighting factors publication 103 recommended of ICRP.

Tissue	ICRP 103
Red bone-marrow	0.12
Colon	0.12
Lung	0.12
Stomach	0.12
Breast	0.12
Gonads	0.08
Bladder	0.04
Liver	0.04
esophagus	0.04
Thyroid	0.04
Skin	0.01
Bone surface	0.01
Brain	0.01
Salivary gland	0.01
Remainder organ*	0.12

*Remainder organ of extrathoracic region, lymphatic nodes and oral mucosa, are approximated by thyroid, muscle and brain.

2.1.4 Factors affecting patient dose [4]

2.1.4.1 Scan Parameters

Kilovolts (kV)

Tube potential is the amount of voltage between an x-ray tube's anode and cathode. It determines the energy of the x-rays emitted. Higher energy x-rays have a greater probability than lower energy x-ray of passing through the body and creating signal at the detector, with all else being equal, higher kV means less noise. However, these high energy x-rays are absorbed by the body, they deposit more energy than lower energy x-rays and therefore, contribute more patient dose. For the same scan parameters, changing the kV from 120 kV to 135 increases the dose by about 33%.

mAs (milliampere-second)

The tube current or mA, determines the number of x-rays the tube produces. Combined with the gantry rotation time, this represents the total x-ray output of the tube per rotation or mAs. Adjustment of the mAs decreased in half will reduce the patient dose by a factor of two.

CT pitch and Helical pitch

Beam pitch is defined as the distance that table travels in a rotation divide by the total active detector width in z direction. Helical pitch is the same except it divided by the individual channel thickness rather than the nominal collimation. By either definition, the higher pitch, the faster table moves through the x-ray beam and, consequently, the lower dose to the patient. MDCT scanners are different from the single slice scanners with respect to pitch. Fig.2.3 shows the effect of different pitch to patient dose. Compared to pitch equal 1 (a), the patient receives lower dose for pitch equal 2 (b) and higher dose for pitch equal 0.5 (c).

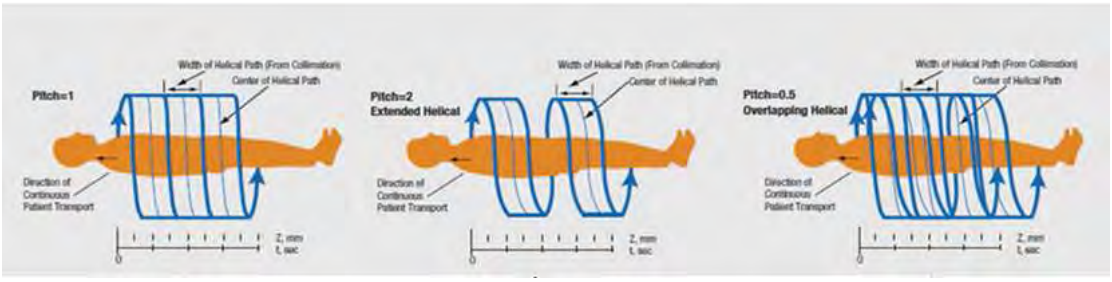

a) Pitch =1 b) Pitch =2 c) Pitch =0.5

Fig. 2.3 The effect of pitch on patient dose.

For the same kV and mAs, higher beam pitch values (>1) spread the x-rays out and reduce dose while lower beam pitch (<1) concentrate the x-ray, increasing the dose.

mAs_{eff} (Effective mAs)

The effective mAs is simply the mAs divided by the pitch. However, since pitch affects the patient dose, mAs by itself does not completely represent the number of x-ray entering the patient. By dividing the standard mAs by beam pitch, a value that is proportional to the patient dose on a given scanner is derived.

$$Effective\ mAs = \frac{mAs}{pitch} \tag{2.8}$$

Collimation

For the multislice scanning, there are many combinations of slice width and number of slices that may be used to acquire the scan volume. With all collimations on multislice system, the actual x-ray beam is slightly wider the nominal beam width. This is to ensure that the detectors on the edge of array receive uniform x-ray coverage, resulting in a small amount of unused radiation called penumbra. The total amount of penumbra is the same regardless of the nominal beam width. Therefore, the larger beams gave the extra radiation from the penumbra.

2.1.4.2 Examination Parameters

Scan length (L)

The local dose, i.e. CTDI, is almost independent of the length of the scanned in body section. The same local dose not hold, however, for the integral dose quantities, i.e. DLP and effective dose. Both increase in proportion to the length of the body section. Therefore, limiting the scan length according to the clinical needs is essential.

Number of scan series

In CT terminology, a scan series is usually refer to as a series of consecutive sequential scans or one complete spiral scan. If the same protocol settings are applied to each series, the local dose will always be the same, while the integral dose is the sum of the DLP or effective dose values of each series. Therefore, it would not make a difference if the body section is scanned as a whole or in several shorter subsections except for overranging effects that will increase proportional to the number of subjections. The multi-phase exams result in an increase in integral radiation exposure that is roughly proportional to the number of phases.

Devices for Automatic Dose Control [5]

The types of AEC used for tube current modulation can be performed using one or more of three basic methods: patient size AEC, z-axis AEC, and rotational AEC. (Fig.2.4)

-Patient-Size AEC and Z-axis AEC

Scan projection radiographs (topographic views) are applied in patient-size and z-axis AEC and are used mainly for the assessment of the size and attenuation of the patient. In patient-size AEC, the tube current is adjusted based on the overall size of the patient to reduce the variation in image quality between small patients and large patients.

-Rotational or Angular AEC

Rotational or angular dose modulation involves varying the tube current to equalize the photon flux to the detector as the x-ray tube rotates about the patient. In angular dose modulation, more dose modulations occur in asymmetric regions and the variation in image noise throughout the examination can be minimized.

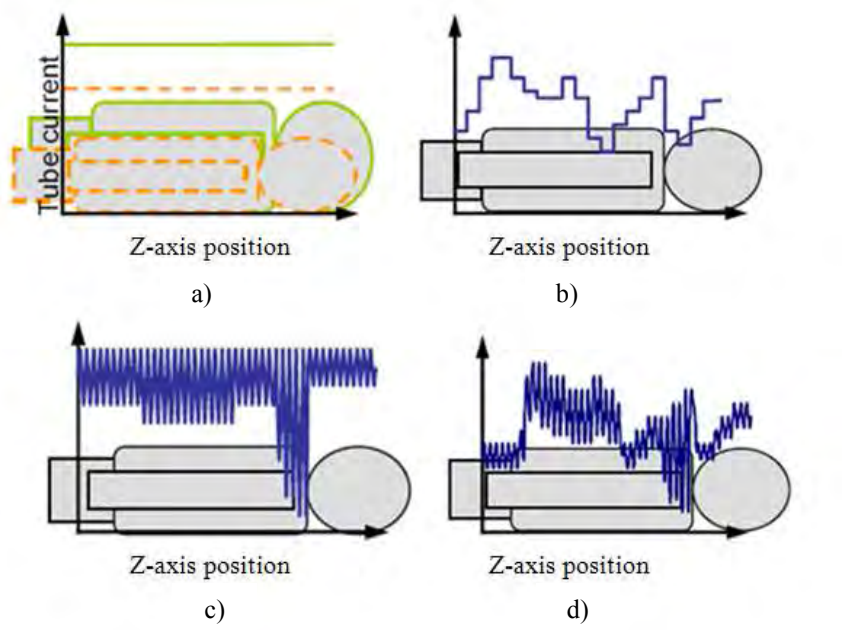

Fig.2.4 Three levels of automatic exposure control. a) patient size AEC b) z-axis AEC c) rotational AEC d) combined effects of using all three levels of AEC.

-Noise Index–based AEC

The current AEC system from GE has two elements: Auto mA provides the patient-size and z-axis AEC elements, and Smart mA provides the rotational AEC element. Users need to understand that image noise is inversely proportional to the square of the tube current. The noise index is used to set the estimated tube current, producing a noise level in reconstructed images that is based on anticipated patient attenuation from topograms. This system also aims to maintain a constant image noise level in each section.

2.1.5 The ImPACT program [6]

2.1.5.1 Introduction

This spreadsheet is a tool for calculating patient organ and effective doses from CT scanner examinations. It makes use of the NRPB (The National Radiological Protection Board) Monte Carlo dose data sets produced in report SR250. SR250 provides normalized organ dose data for irradiation of a mathematical phantom by a range of CT scanners. As SR250 was produced in 1993, it does not include data for more modern scanners. To overcome this problem, physicists in the United Kingdom

and Europe carried out the ImPACT CT scanner dose survey. This work provides a method for 'matching' the dose distribution of newer scanners to scanners included in SR250. The matching results are included in this spreadsheet. As new scanners are introduced, their matches will be included in updates to this spreadsheet.

2.1.5.2 Worksheet

CT Dosimetry calculation program consists of 12 worksheets as shown in Fig.2.5.

1. Introduction: Provides an introduction and instructions to use
2. Scan Calculation: Selects data entry and shows results sheet
3. Pediatric: Inform relative doses to adult and pediatric patients
4. Phantom: Allows interactive selection of the scan range used for dose calculation using a diagram of the phantom used to generate SR250
5. Scanners: Provides data on CT scanner models, including CTDI in air and phantom, as well as the scanner matching data
6. Match Data: Gives data required to perform the scanner matching in the Scanners worksheet
7. Collimation: Lists relative CTDI values at different collimations for a range of CT scanners. These values are more useful for multi-slice scanners, as the CTDI can vary considerably over the range of available collimations
8. Monte Carlo Data: Contains the unformatted SR250 data set
9. Doses: Contains the formatted dose data from the SR250 data set that is currently loaded
10. Dose Calculations: Performs the organ dose calculations, and calculation of remainder organ doses etc.
11. Selections: Provides data for the drop down selection boxes in the Scan Calculation worksheet, and performs calculations for 'remainder' organ doses
12. Version: Details the changing in each version, from version 0.99e onwards

There are also a number of Visual Basic macros used by CTDosimetry, held in the modules Phantom Diagram, Scanner Selection and Update Data Set.

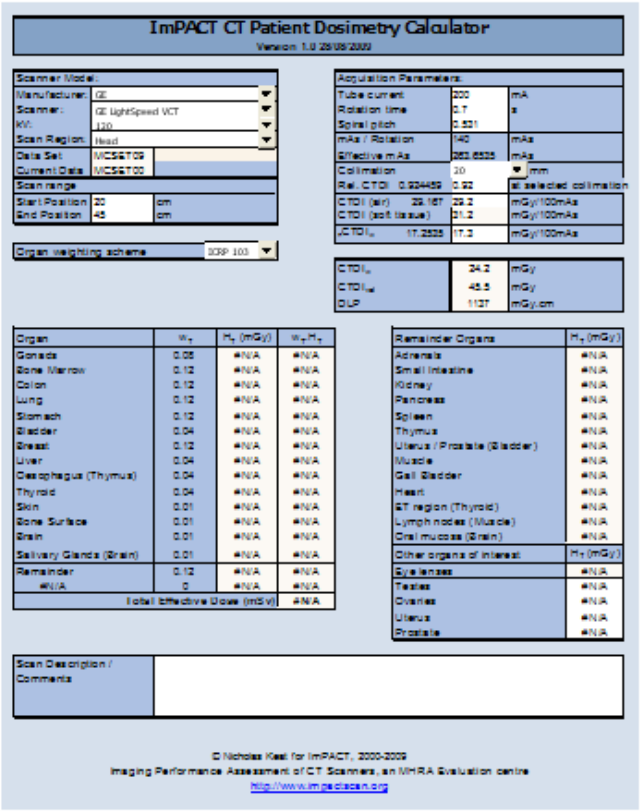

Fig.2.5 The ImPACT Patient Dosimetry Calculction Program.

2.1.5.3 Using CT Dosimetry Calculator

To calculate doses using CTDosimetry.xls, the user must enter a number of parameters relating to the scanner and the scan series. The following four selections, made in the top left box on the Scan Calculations worksheet defined the Monte Carlo data set that is used:

1. Manufacturer: Select the scanner manufacturer from the drop down list
2. Scanner: Select the scanner model or scanner model group for the drop down list
3. kV: Choose the appropriate scan kV
4. Scan Region: Choose head or body

The Monte Carlo data set that is used for this combination of scanner, kV and body part is displayed in the cell marked 'Data Set'. The data set that is currently loaded is displayed below. If these do not match, no dose is calculated. To load the appropriate data set, and enable dose calculation, press the 'Update Data Set' button.

5. Tube current: The x-ray tube current. Note that this should be the actual scanner mA, and not the 'effective mAs' displayed on some multi-slice scanners
6. Rotation time: The scanner tube rotation time
7. Spiral pitch: The scanning pitch (table travel per rotation/total collimated slice width). For axial scanning, (couch increment)/ (collimated slice width) should be used
8. mAs/rotation: Do not enter data in this box (it is calculated automatically)
9. Effective mAs: The mAs/per rotation divided by the spiral pitch. This is a calculated value that provides a basis for comparison of spiral protocols with different pitches
10. Collimation: The total nominal x-ray beam width along the z-axis, selected from a range of possible values in the drop down box. This determines the relative CTDI compared to the reference (usually 10 mm) collimation
11. Rel. CTDI: The CTDI at the selected collimated x-ray beam thickness, relative to the CTDI at the reference collimation (usually 10 mm)
12. CTDI (air): The free in air $CTDI_{100}$ value (in mGy/100mAs), as defined in EUR 16262: European Guidelines on Quality Criteria for Computed Tomography, pub. European Commission. CTDI values for most of the scanners are listed on the Scanner Worksheet. Pressing the 'Look up' button will enter the value in this cell. The value in this cell is corrected for the relative CTDI value in the cell above
13. CTDI (soft tissue): The CTDI to ICRU muscle, used as an approximation to the dose to soft tissue within the body. This is the CTDI(air) x 1.07 for CT scanner energies
14. ${}_{n}CTDI_{w}$: Weighted CTDI measured in a standard CTDI phantom (normalisedfor 100 mAs)

$$nCTDI_w = (CTDI_{center} + 2CTDI_{periphery})/3 \qquad \text{(EUR16262)}$$

15. $CTDI_w$: Weighted CTDI measured in a standard CTDI phantom.

$$CTDI_w = (CTDI_{center} + 2CTDI_{periphery})/3 \qquad \text{(EUR16262)}$$

16. $CTDI_{vol}$: Volumetric CTDI, given by

$$CTDI_{vol} = CTDI_w / Spiral\ Pitch$$

17. *DLP*: Dose Length Product, given by

$$DLP = CTDI_{vol} \times Scan\ length$$

18. Start Position: The start position of the scan series. The diagram on the Phantom worksheet shows the position of the phantom's organs relative to the number scale, which is 0 at the base of the trunk in example. This value can be entered manually in the worksheet, or can be taken from the shaded area on the Phantom worksheet diagram. This can be adjusted using the up and down arrows. Pressing the 'Get from Phantom Diagram' button enters these values into the start and end position boxes in Scan Calculation.
19. End Position: The end position of the scan series - Note that this should include the slice thickness, so, for example, a single 5mm slice 20cm from the base of the trunk would have a start position of 20, and an end position of 20.5cm. Start and End position values are interchangeable.
20. Organ weighting scheme: The calculation of effective dose is governed by the weighting of doses to individual organs according to tissue weighting factors given in ICRP publications 60 and 103. Changing this value alters the organ weighting factors and organs used in effective dose calculation.

When the above values are entered, the doses to each of the individual organs, as defined by the SR250 data set appear in the cells below the scan parameters. These are combined according to the tissue weighting factors given in ICRP publications 103, to calculate an effective dose. In addition, the weighted CTDI ($CTID_w$), volume CTDI ($CTDI_{vol}$) and dose length product (DLP) are also displayed. Note that not all of the organs listed in ICRP publication 60 and 103 are included in NRPB SR250. In order to approximate dose to the esophagus, salivary gland and prostate, the thymus, brain and bladder doses are used. The dose for muscle is approximated from the total body dose - dose to all other organs and contents. Three organ doses included in the ICRP 103 definition of remainder organ; extrathoracic region, lymphatic nodes and oral mucosa, are approximated by thyroid, muscle and brain.

2.1.6 Thermoluminescent dosimetry [7]

Thermoluminescent (TL) is defined as a phenomenon of the visible photons released by thermal, and this characteristic was used for radiation dosimeter, the phenomenon is shown in Fig.2.6.

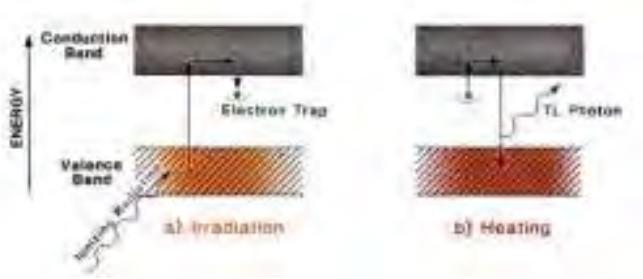

Fig.2.6 A simplified energy level diagram of thermoluminescence process.

The TLDs which present the small size, good energy dependence, good sensitivity and large useful dose range of TLDs are key advantages. Many crystalline materials exhibit the event of thermoluminescence used in TLDs. As the direct measurement of dose is possible under conditions in which other forms of dosimetry are not practically.

There are several thermoluminescence phosphors available but the most noteworthy are lithium fluoride (LiF), lithium borate ($Li_2B_4O_7$), and calcium fluoride (CaF_2). Of these phosphors, LiF is most extensively studied and most frequently used for clinical dosimetry. LiF in its purest form exhibits relatively little thermoluminescence. But the presence of a trace amount of impurities (e.g., magnesium) provides the radiation-induced thermoluminescence. These impurities give rise to imperfections in the lattice structure of LiF and appear to be necessary for the appearance of the thermoluminescence phenomenon, this study used the TLDs-100 crystal doped with magnesium and titanium (LiF:Mg,Ti)) for the organ dose measurement in Rando phantom.

TLD-100 is a type of radiation dosimeter that measures the ionizing radiation exposure. Before they are used, TLDs need to be annealed to erase the residual signal.

A basic TLD reader system [8] consists of a planchet for placing and heating the TLD, a PMT for detecting the thermoluminescence light emission and converts it into an electrical signal linearly proportional to the detected photon fluence and an electrometer for recording the PMT signal as a charge or current it is shown in Fig.2.7.

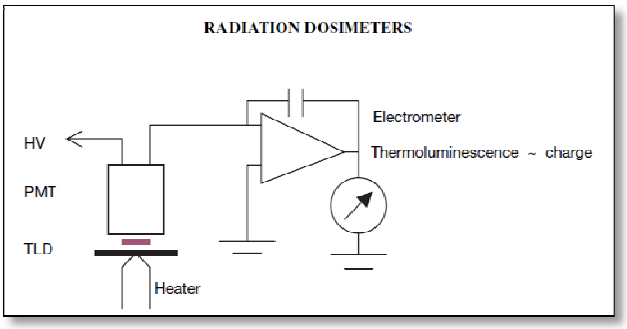

Fig.2.7 Diagram of TLD reader.

The thermoluminescence intensity emission is a function of the TLD temperature. Keeping the heating rate constant makes the temperature proportional to time, and so the thermoluminescence intensity can be plotted as a function of temparature if a recorder output is available with the TLD measuring system. The resulting curve is called the TLD glow curve which is shown in Fig.2.8. The total thermoluminescence signal emitted can be correlated to dose.

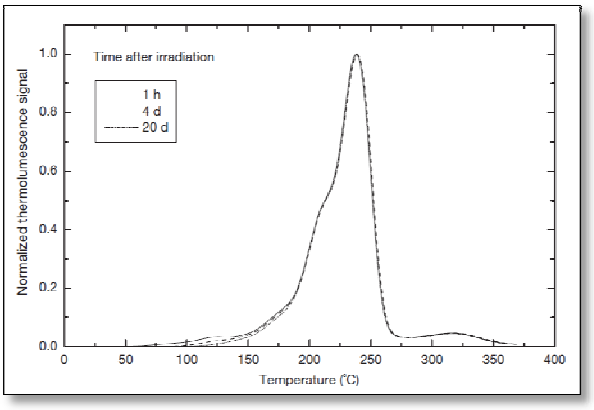

Fig. 2.8 A typical thermogram (glow) of LiF:Mg,Ti measured with a TLD reader at a low heating rate.

The arrangement for measuring the thermoluminescence output is shown schematically in Fig.2.9. The irradiated material is placed in a heater cup or planchet, where it is heated for a reproducible heating cycle. The emitted light is measured by a photomultiplier tube (PMT) which converts light into an electrical current. The current is then amplified and measured by a recorder or a counter.

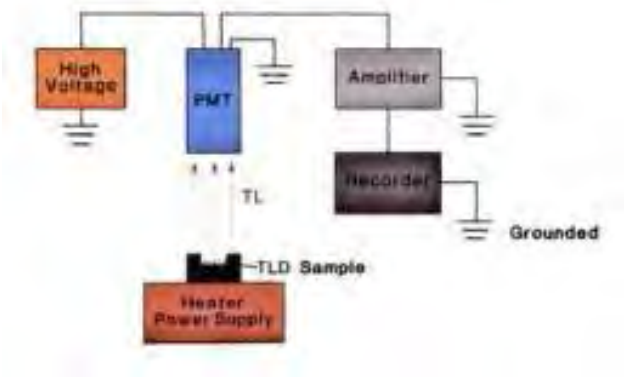

Fig.2.9 Schematic diagram apparatus for thermoluminescence dose measurement.

2.1.6.1 Calibration of thermoluminescent dosimeters [9]

The purpose of calibrating a TLD instrument is to produce consistent and accurate reading in dosimetrically meaningful units. The calibration process involves the following 3 steps.

A) Generate calibration dosimeter

In this process, an element correction coefficient (ECC) is generated by using a set of dosimeters, typically 1-2% of the total population to be calibration dosimeters. They are identified and segregated from the field dosimeters. All dosimeters are annealed to clear them all residual exposure. Duration time between annealing and exposing should be the same for all dosimeters. After being exposed to the known radiation dose, the charge integral value (Q_i) in nanocoulomb (nC) of each dosimeter

(i) is read out and recorded. Then the average charge integral $\bar{Q}$ of all dosimeters is calculated and the element correction coefficient (ECC_i) for individual dosimeter i (i = 1, 2, 3,…, n) is computed by dividing the average charge integral by the individual charge (Q_i) as:

$$ECC_i = \frac{\bar{Q}}{Q_i} \quad (2.9)$$

B) Calibration of TLD reader

A group of dosimeters about 1 – 2 % of dosimeters in (A) which have ECC_i value close to 1 are chosen to be calibration dosimeters. The calibration dosimeters are exposed to known amount of radiation dose (D) in grays and read by TLD reader. As (Q_i) is the reading for the dosimeter i, the corrected charge integral (Q_i) of the dosimeter is calculated by:

$$Q_{ci} = Q_i \times ECC_i \quad (2.10)$$

Then the reader calibration factor (RCF) is calculated from the equation:

$$RCF = \frac{Q_c}{D} \quad (2.11)$$

When $Q_c$the average is corrected charge integral and calculated by:

$$Q_c = \frac{1}{n}\sum_{i=1}^{n} Q_i \quad (2.12)$$

C) Calibration of dosimeter

The rest of the dosimeter [number of the dosimeters in (A) – number of dosimeters in (B)] is used as field dosimeters. They are exposed by the known radiation dose of D grays and read by TLD reader. The calibration value of element correction coefficient for individual dosimeter (ECC_{ci}) is then calculated by:

$$ECC_{ci} = \frac{RCF \times D}{Q_i} \quad (2.13)$$

2.1.6.2 Determination of unknown radiation dose

The field dosimeters in 2.13 (C) are used to measure unknown radiation dose. The unknown dose D in Grays is calculated by using ECC_{ci} from the equation:

$$D = \frac{Q_i \times ECC_{ci}}{RCF} \quad (2.14)$$

2.2 Review of related literatures

Calzado A et al [10] determined organ doses from a set of frequent third generation CT examinations by the measurements in a physical anthropomorphic phantom by using TLD dosimeters which calibrated by ^{137}Cs source and compared with the calculation by Monte Carlo techniques using mathematical phantoms and CT regional survey doses under the same examination techniques based on protocol of Phillips Tomoscan TX scanner at 120 kV. The result showed the eye lenses doses during head examination were 32.2 mSv, 35.6 mSv and 29.0 mSv for measured, calculated and deduced from the survey, respectively. For head examination, effective dose was 1.07 mSv, 1.14 mSv, 1.08 mSv for measurement, calculation and survey, respectively. For chest examination, effective dose was 4.30 mSv, 5.58 mSv, 5.57 mSv for measurement, calculation and survey, respectively. For abdomen examination, effective dose was 14.5 mSv, 11.6 mSv, 8.03 mSv for measurement, calculation and survey, respectively. For pelvis examination, effective dose was 12.7 mSv, 13.7 mSv, 6.81 mSv for measurement, calculation and survey, respectively. The uncertainty of average organ and effective doses estimated from the measurement ranged from about 10% for small and superficial organs to more than 20% for the internal larger organs, such as liver or lung. In the case of calculations, the overall uncertainties of average organ doses were 18 -25% and estimated from the survey was larger difference in abdomen and pelvis CT examination when they compared with measurement and calculation.

Fujii K et al. [11] studied the evaluation of organ and effective doses to patients undergoing routine adult and pediatric CT examinations with 64-slice CT scanners and compared the doses between the 4, 8, and 16 multislice CT scanners. Patient doses were measured with small silicon photodiode dosimeters, which were implanted at various tissue and organ positions within adult and 6-year-old child anthropomorphic phantoms. Output signals from photodiode dosimeters were read on a personal computer, from which organ and effective doses were computed. For the adult phantom, organ doses (for organs within the scan range) and effective doses were 8–35 mGy and 7–18 mSv, respectively, for chest CT, and 12–33 mGy and 10–21 mSv, respectively, for abdominopelvic CT. For the pediatric phantom, organ and effective doses were 4–17 mGy and 3–7 mSv, respectively, for chest CT, and 5–14 mGy and 3–9 mSv, respectively, for abdominopelvic CT. Doses to organs at the boundaries of the scan length were higher for 64-sliceCT scanners using large beam widths and/or a large pitch because of the larger extent of over-ranging. The $CTDI_{vol}$, DLP and the effective dose values using 64 slice CT for the adult and pediatric phantoms were the same as those obtained using 4, 8 and 16 slice CT. Conversion factors of DLP to the effective dose by ICRP 103 were 0.024 $mSv \cdot mGy^{-1} \cdot cm^{-1}$ and 0.019 $mSv \cdot mGy^{-1} \cdot cm^{-1}$ for adult chest and abdominal pelvic CT scans, respectively.

Lo GG, et al [12] compared the effective dose for patient undergoing new-generation computed tomography and 64 slice GE VCT MDCT using protocol of manufacture setting. Patient dose estimated as the product of the measured dose-length product and the corresponding conversion coefficient for each type of scan. The results showed the average radiation dose of 1.9 mSv for brain, 6.9 mSv for thorax, 13.4 mSv for abdomen biphasic, 20.9 mSv for abdomen triphasic, and 9.3 mSv for urogram scans. For 64-slice MDCT, they were 3.4 mSv for brain, 24.7 mSv for thorax, 38.9 mSv for abdomen biphasic, 53.9 mSv for abdomen triphasic, and 18.3 mSv for urogram scans. The effective doses of new-generation computed tomography delivered a significantly lower radiation dose to patients than with 64-slice MDCT.

Ngaile JE, et al. [13] determined the radiosensitive organs doses undergoing CT examinations of Philips Medical Systems Tomoscan SR 4000, Tomoscan M-EG, Siemens Medical Systems Somatom Plus 4, Somatom AR Star, GE Medical Systems CT/e, CT Max 640 scanners and assessed CT scanning protocols in practice. The mean organ doses in their study for the eye lenses (for head), thyroid (for chest), breast (for chest), stomach (for abdomen), and ovary (for pelvis) were 63.9 mGy, 12.3 mGy, 26.1 mGy, 35.6 mGy, and 24.0 mGy, respectively. These values were mostly comparable to and slightly higher than the results with other studies, that reported from the literature for the United Kingdom, Japan, Germany, Norway, and the Netherlands because of the larger scan length of examination.

Tsapaki V, et al. [14] measured the radiation doses of head, chest, and abdomen examination and compared the results with the diagnostic reference levels, as part of the International Atomic Energy Agency (IAEA) Research coordination project. All scanners were helical single-section or multidetector CT systems, data was collected included patient height, weight, sex, and age; tube voltage and tube current–time product settings; pitch; section thickness; number of sections; weighted or volumetric CT dose index; and dose-length product (DLP). The effective dose was estimated and serving as collective dose estimation data. Mean $CTDI_{vol}$ and DLP were 39 mGy and 544 mGy.cm, respectively, for head CT; 9.3 mGy and 348 mGy.cm, respectively, for chest CT; and 10.4 mGy and 549 mGy.cm, respectively, for abdominal CT. These results were lower than the European diagnostic references levels values. The effective dose estimate was determined by using DLP measurement multiply with normalized coefficients found in the European guidelines for CT. The summary of result of effective doses was 1.2 mSv for head, 5.9 mSv for chest, and 8.2 mSv for abdomen. The newer scanners have improved technology that facilitates lower patient doses.

Brenner DJ, et al. [15] studied the increasing number of CT scans, the associated radiation doses, and the consequent cancer risks in adults and particularly in children. Although the risks for any one person are not large, the increasing exposure to radiation in the population may be a public health issue in the future. The authors determined that CT involved larger radiation doses than the more common conventional x-ray imaging procedures. The organ dose determined the level of risk to the organ, the estimated organ doses were 15 millisieverts (mSv) in adult and 30 millisieverts (mSv) in neonate for single CT scan, with an average of two to three CT scans per study. The data of atomic-bomb survivors, who received low doses of radiation, illustrated the radiation dose range from 5 to 150 mSv and the mean dose was about 40 mSv. The organ dose of epidemiologic study resulted in the dose range of 30 to 90 mSv. The organ doses of both atomic-bomb survivors and epidemiology were approximated the relevant organ dose from a typical CT study involving two or three scans in an adult.

CHAPTER III

RESEARCH METHODOLOGY

3.1 Research design

This study is an observational cross-sectional study.

3.2 Research design model

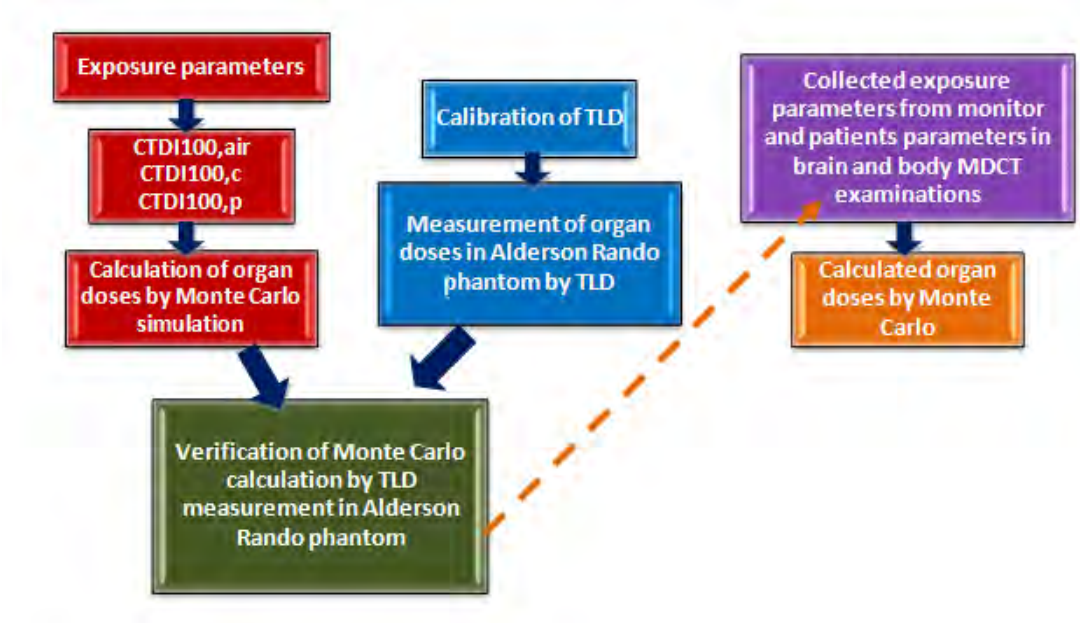

Fig 3.1 Research design model.

3.3 Conceptual frameworks

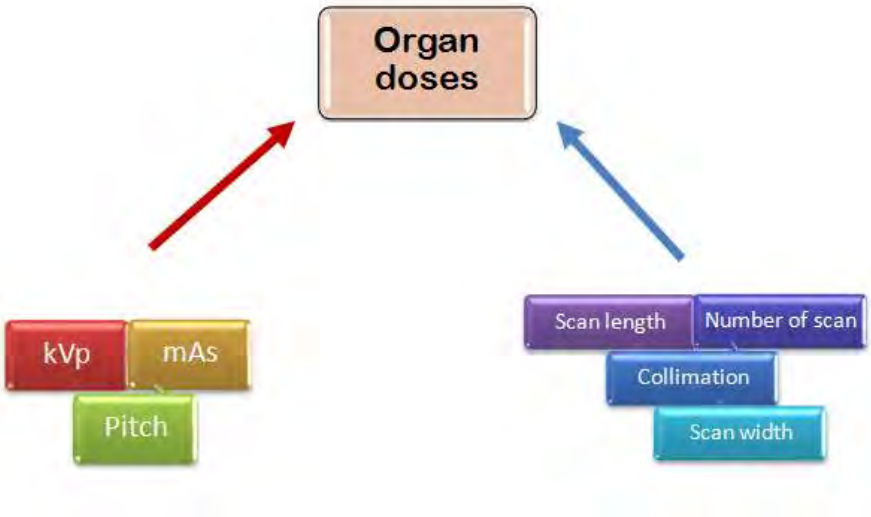

Fig. 3.2 Conceptual frameworks.

3.4 Keywords

Organ dose
Multidetector Computed tomography
Monte Carlo simulation
Thermoluminescent dosimetry

3.5 Research question

What are the average organ doses attribute from brain and body Multidetector Computed Tomography?

3.6 Sample size determination

3.6.1 Target population

The patients underwent 64 slices MDCT at department of Radiology, Rajavithi Hospital.

3.6.2 Eligible criteria

Inclusion criteria

The out-patient of over 20 year old who was scanned in brain, chest and abdomen examinations.

Exclusion criteria

The in-patient and out-patient of under 20 year old.

3.6.3 Calculation of sample size

Sample sizes from 30 cases of pilot study are calculated from continuous data based on the formula and construct 95 % (CI) confidence interval ($\alpha = 0.05$, $Z_{\alpha/2} = 1.96$)

$$n = \frac{Z^2_{\alpha/2} \times \sigma^2}{d^2} \quad (3.1)$$

Sample size of chest examination

σ = SD (standard deviation from mean) = 31.65 ± 7.32 cm
d = Acceptable error of scan length 2 cm

$$n = \frac{(1.96)^2 \times (7.32)^2}{(2)^2}$$

n = 53 cases

Sample size of abdomen examination

σ = SD (standard deviation of average) = 36.50 ± 7.45 cm

d = Acceptable error of scan length 2 cm

$$n = \frac{(1.96)^2 \times (7.45)^2}{(2)^2}$$

n = 53 cases

Sample sizes for brain scans, there are less different in scan length, the calculated sample size is very small. However, the same sample size with chest and abdomen will be collected.

3.7 Materials

3.7.1 The computed tomography equipment

The 64 slices MDCT scanner (LightSpeed, VCT, General Electric Medical Systems, Waukesha, WI, USA) is shown in Fig. 3.3 with maximum kV and mA at 140 and 700, respectively. The machine was installed in 2007, at department of Radiology, Rajavithi Hospital. The summary of machine specification is shown in Table 3.1.

Fig. 3.3 The computed tomography equipment.

Table 3.1 Summary of 64 slice LightSpeed GE VCT computed tomography.

Scanner gantry	The technique and application specification data.
Scanner type	64 slices, 3rd generation
Gantry aperture	70 cm
Gantry tilt – Sequential / Helical	± 30 degrees
X-ray generator tube and tube	
Power rating	85 kW
Anode heat capacity	8 MHU
Maximum anode cooling rate	2100 KHU/min
Detection system	
Detector type	Solid state
Detector array configuration	64 x 0.625 mm width
Maximum z-axis coverage	40 mm
Maximum z-axis coverage with sub-mm slices	40 mm
Couch	
Length and width	285 x 42 mm
Maximum scannable range	70 medium table, 200 long table
Maximum height out of gantry	43 cm
Maximum weight on couch	227 kg
Scan parameters	
Minimum rotation time in helical mode	0.4 sec
Kilovoltage setting	80, 100, 120, 140 kVp
Tube current range at 120 / 130 kV	10 – 700 mA
Image reconstruction	
Reconstruction field of view range	9.6 – 50 cm
Reconstruction matrix	512 x 512
Reconstruction rate for standard head scan 5122	16 images / sec
Reconstruction rate for standard body scan 5122	Up to 6 images / sec
Dose reduction features	
Tube current modulation (x-y and z)	(x-y and z)
Adaptive collimators in helical scanning	No
Data management and connectivity	
Standard total hard disc capacity	584 GB
Ability to burn images to disc	Yes
Rate to image transfer: scanner to workstation	Up to 16 images / sec
IHE schedule workflow supported	Yes
Manufacture' s performance data	
Scan plane limiting clinical spatial resolution	0.35 (14.2 lp/cm @ 4%MTF)
Longitudinal (z-axis) limiting clinical spatial resolution	0.35 (14.2 lp/cm @ 4%MTF)
Maximum height out of gantry	43 cm

Table 3.1 Summary of 64 slice LightSpeed GE VCT computed tomography. (Continued)

Scanner gantry	The technique and application specification data.
Manufacture's performance data	
Contrast resolution: smallest rod size discernable (mm @ 0.3% contrast @ x mGy surface dose in Catphan	3 mm@ 0.3% 22.2 mGy $CTDI_{vol}$
$CTDI_w$ for standard head scan (mgy/100mAs) *Do not use for direct dose comparisons	19.3 @ 120 kV
$CTDI_w$ for standard body scan (mgy/100mAs) *Do not use for direct dose comparisons	8.6 @ 120 kV
Power requirements	
Power requirements (gantry)	3 phase, 380-480 V, 150 kVA
Minimum floor load-bearing	1448 kg/m^2

*This table does not reflect the scanner's dose efficiency. A relative patient dose at the stated kV can be calculated using this data in conjunction with the recommended clinical scan parameter (mAs, pitch).

3.7.2 The pencil ionization chamber

The 100 mm long pencil ionization chamber (DCT 10-RS RTI Electronics AB, Molndal, Sweden) is shown in Fig. 3.4. It is 4.9 cm^3 active volumes, 10 cm total active length, 0.8 cm inner diameter of outer electrode, and 0.1 cm diameter of inner electrode. It is connected with the electrometer during the measurement.

Fig. 3.4 The pencil ionization chamber.

3.7.3 The electrometer

The electrometer (Type SOLIDOSE 400, RTI Electronics AB, Molndal, Sweden) is shown in Fig. 3.5, its leakage is within $4x10^{-15}$ Amperes for 80 -150 kV radiation quality, and the calibration factor $N_{D,K}$ equals to 24.2 mGy cm/nC (120 kV/HWD 4.05 mmAl).

Fig. 3.5 The electrometer.

3.7.4 Monte Carlo simulation program

Dose estimation methodology was based on the NRPB (The National Radiological Protection Board) SR-250 Monte Carlo simulations. The exposure factors were entered into the ImPACT (Imaging Performance Assessment of CT scanners) spreadsheet shown in Fig.3.6, along with CTDI which the measurements made with an ionization chamber. The spreadsheet used these data and table of normalized organ doses to estimate the organ dose by matching with the manufacturer CT machine.

ImPACT CT Patient Dosimetry Calculator
Version 1.0 28/08/2009

Scanner Model:			
Manufacturer:	GE		
Scanner:	GE LightSpeed VCT		
kV:	120		
Scan Region:	Body		
Data Set	MCSET20	Update Data Set	
Current Data	MCSET00		
Scan range			
Start Position	20	cm	Get From Phantom Diagram
End Position	45	cm	

Organ weighting scheme	ICRP 103

Acquisition Parameters:			
Tube current		330	mA
Rotation time		0.6	s
Spiral pitch		1.375	
mAs / Rotation		198	mAs
Effective mAs		144	mAs
Collimation		40	mm
Rel. CTDI	Look up	0.86	at selected collimation
CTDI (air)	Look up	27.1	mGy/100mAs
CTDI (soft tissue)		29.0	mGy/100mAs
$_nCTDI_w$	Look up	9.0	mGy/100mAs

$CTDI_w$	17.7	mGy
$CTDI_{vol}$	12.9	mGy
DLP	323	mGy.cm

Fig. 3.6 The ImPACT spreadsheet.

3.7.5 The PMMA (Polymethyl methacrylate acrylic) phantom

The head and body phantom is shown in Fig. 3.7. There are 16 cm of head and 32 cm of body diameter CTDI PMMA phantom. The 10 cm long CT pencil ionization can be placed in the holes of phantom.

Fig. 3.7 The head and body PMMA phantom.

3.7.6 The Alderson Rando phantom

The Alderson Rando phantom which is shown in Fig. 3.8 incorporates materials to simulate various body tissue-muscle, bone, lung, and air cavities. It is made of tissue equivalent material based on a synthetic isocyanate rubber. The phantom material is processed chemically and physically to achieve a density of 0.985 g/cm^3 and an effective atomic number of 7.3 based on the International Commission on Radiation Units and Measurement (ICRU) [16].

The phantom is shaped into a human tarso and is sectioned transversely into slices of 2.5 cm each containing a matrix of 0.5 cm diameter holes spaced 3 cm a part. The lungs and cavities are molded of an air-expanded version of the soft tissue material having a density of 0.3 g/cm^3 and an effective atomic number is the same as soft tissue [17].

Fig. 3.8 The Alderson Rando phantom.

3.7.7 The thermoluminescent dosimeter

The TLD used in this study is LiF crystal doped with magnesium and titanium (LiF:Mg,Ti). It is known as TLD-100, it consists of Li-6 (7.5%) and Li-7 (92.5%). The TLDs have a nominal density of 2.64 g/cm^3 and effective atomic number (Z_{eff}) of 8.2, a value close to tissue. TLD chips with the dimension of 3.2 mm x 3.2 mm x 0.89 mm are used for this study. They are shown in Fig. 3.9a. The three pieces of TLD chips were loaded into the plastic tubes, shown in Fig.3.9b. These tubes with TLDs were irradiated for TLD characteristic study and dose measurement.

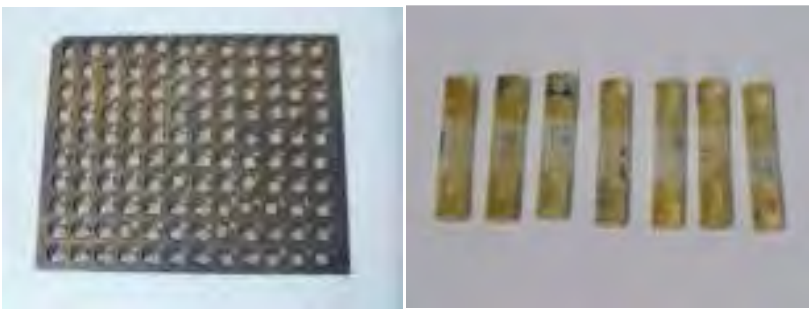

a) b)

Fig. 3.9 The TLDs and plastic tubes.
a) The pieces of TLD chips b) The tubes with TLDs

3.7.8 The automatic TLD reader [9]

The Harshaw model 5500 automatic TLD reader is shown in Fig. 3.10, it is a personal computer driven, tabletop instrument for TLD measurement. This reader is capable of reading 50 diameters per loading and accommodates TLD chips, rods and cubes in a variety of sizes. The reader uses hot nitrogen gas heating with a closed loop feedback system that produces linearly ramped temperatures accurate within ± 1^{o}c to 400^{o}c. Nitrogen is routed through the PMTchamber to eliminate condensation.

Fig. 3.10 The automatic TLD reader.

3.7.9 The Cobalt-60 teletherapy machine

The THERATRON 80 ^{60}Co teletherapy machine is shown in Fig. 3.11. The ^{60}Co machine was used for TLD sensitivity determination due to the constant emission of the radiation.

Fig. 3.11 The THERATRON 80 ^{60}Co teletherapy machine.

3.8 Methods

The study was performed in department of radiology at Rajaviti Hospital. This study carried out into two parts:

Part 1: The organ, effective dose calculation and measurement in Alderson Rando phantom

1.1 Monte Carlo simulation method in Alderson Rando phantom
1.2 Thermoluminescent dosimetry method in Alderson Rando phantom

Part 2: The organ and effective dose calculation in patient

2.1 Monte Carlo simulation method in patient

The quality control of the 64 slice GE VCT MDCT equipment was undertaken before performing the dose measurements. The procedures and results are shown in appendix B.

3.8.1 Part 1: The organ, effective dose calculation and measurement in Alderson Rando phantom

3.8.1.1 Monte Carlo simulation method in Alderson Rando phantom

Computed tomography dose index measurement

The dose measurements were performed for brain and body protocol using axial scan, 120 kV, 100 mA, 1 sec., 10 mm interval, 10 mm slice thickness, small head FOV.

A) The pencil ionization chamber which connected to the electrometer was placed in air at the isocenter of gantry. It is shown in Fig.3.12.

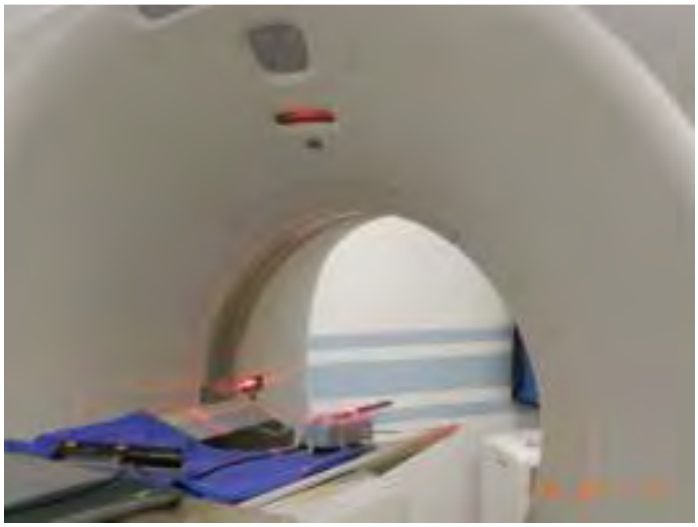

Fig. 3.12 The pencil chamber at the isocenter in air.

B) The pencil ionization chamber was placed at the center of the head and body phantom. It is shown in Fig. 3.13.

a) b)

Fig. 3.13 The pencil chamber at the center of the head and body phantom.
a) head phantom b) body phantom

C) The pencil ionization chamber was placed at the peripheries of the head phantom. It is shown in Fig. 3.14, a) at 12 o'clock, b) at 3 o'clock, c) at 6 o'clock, d) at 9 o'clock.

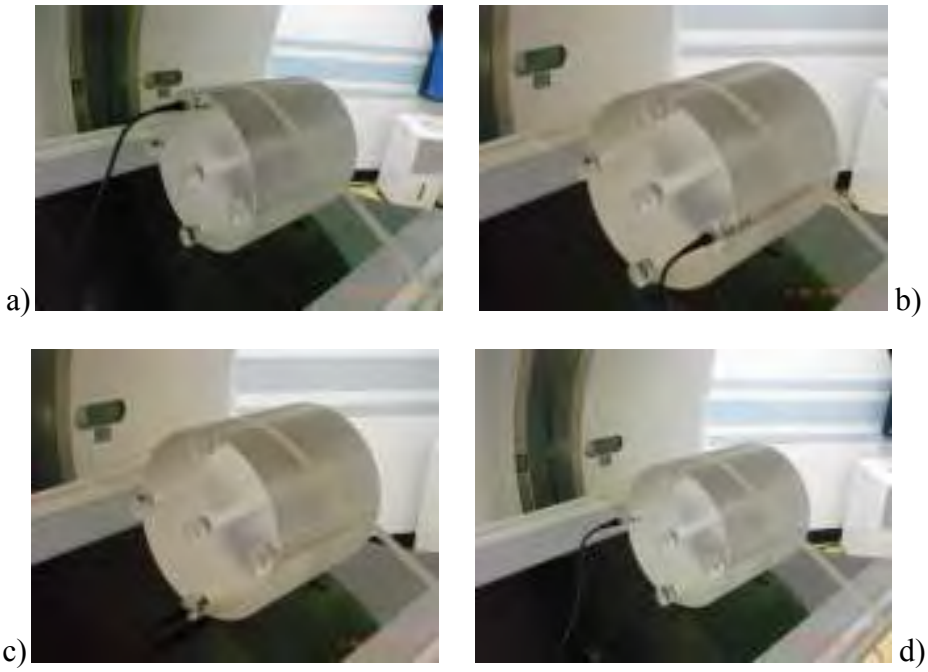

Fig. 3.14 The pencil ionization chamber at the peripheries of the head phantom.

D) The pencil ionization chamber was placed at the peripheries of the body phantom. It is shown in Fig. 3.15, a) at 12 o'clock, b) at 3 o'clock, c) at 6 o'clock, d) at 9 o'clock.

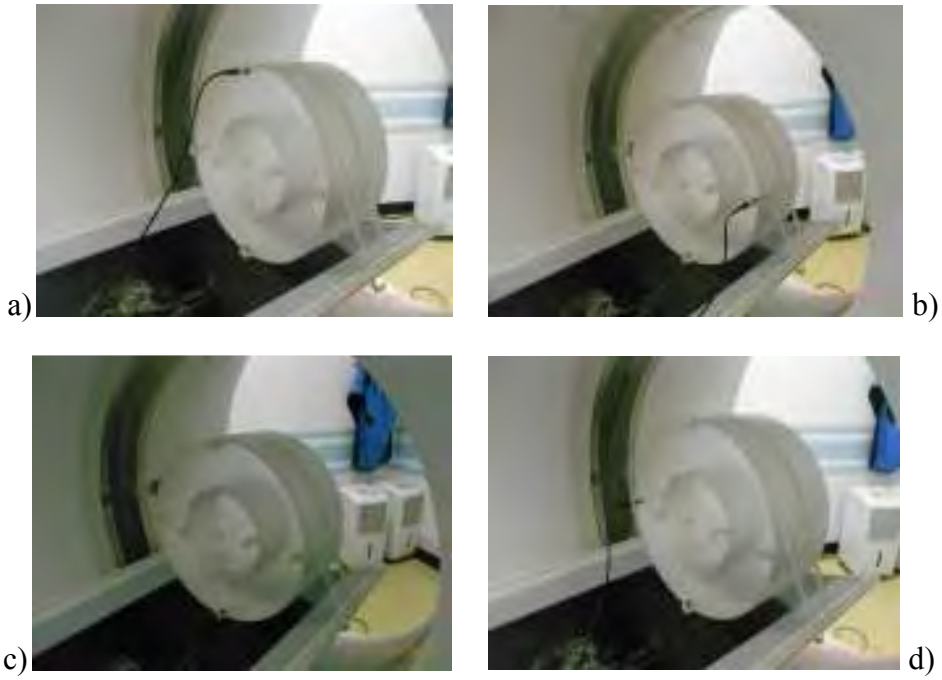

Fig. 3.15 The pencil ionization chamber at the peripheries of the body phantom.

The organ and effective dose calculation in Alderson Rando phantom

The ImPACT Program shown in Fig. 3.16 is a tool for calculating organ and effective doses from CT scanner examinations. The CTDI values at center and the average value at periphery of the PMMA phantom together with exposure parameters, type and model of CT were put into the ImPACT Calculator Program version 1.0 in order to calculate organ and effective doses. The ImPACT CT software package coupled organ weighting factors of International Commission on Radiological Protection (ICRP) publication 103.

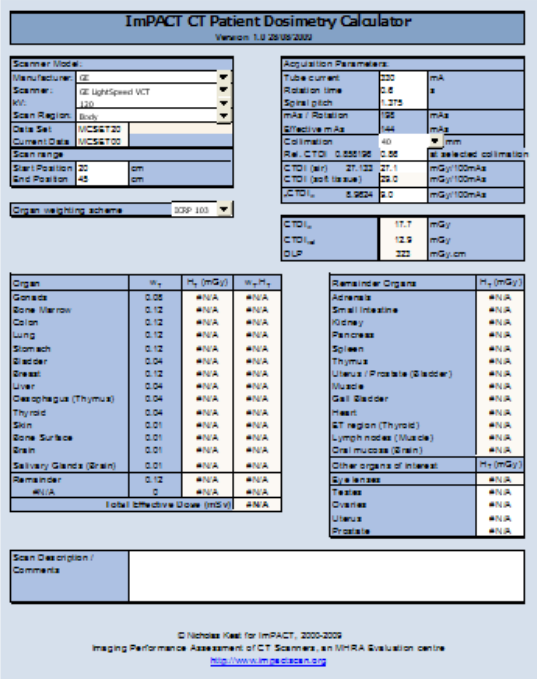

Fig. 3.16 The ImPACT CT Patient Dosimetry Calculator Program.

The setting parameters of protocol employed in brain, chest and abdomen examination are shown in Table 3.2 and slice thickness was 5 mm in all protocols.

Table 3.2 The exposure parameters of the CT protocols used for CT scanning in Alderson Rando phantom**.**

Protocol	kV	mA	Rotation time (sec)	Pitch (mm/rotation)	Collimation (mm)	Scan length (cm)
Brain	120	200	0.7	0.531	20	14.5
Chest	120	Smart mA (200 - 300)	0.6	1.375	40	41
Abdomen	120	Smart mA (200 - 400)	0.6	0.984	40	40

Brain protocol: Ref. noise index 3.80, HVL (head filter) 6.3 mmAl.
Chest and abdomen protocols: Ref. noise index 11.57 and HVL (body filter) 7.5 mmAl.

3.8.1.2 The organ and effective dose by TL dosimetry method in Alderson Rando phantom

TLD preparation

A) Sensitivity

The sensitivity of each dosimeter was determined by exposing 5 cGy of ^{60}cobalt (gamma-ray) to 120 dosimeters. The parameters were set to irradiate at 80 cm source-axis distance (SAD), 10 cm depth of the virtual water slab phantoms of 30x30 cm^2 size including TLD expose box 1.2 cm thickness, no wedge, 12x12 cm^2 field size, and 0.09 min exposure time. The procedure is shown in Fig. 3.17.

The charge integral value of each dosimeter was read and the ECC was calculated according to equation 2.9. The dosimeters that have the ECC values between 0.9 and 1.1 were selected for using in this study.

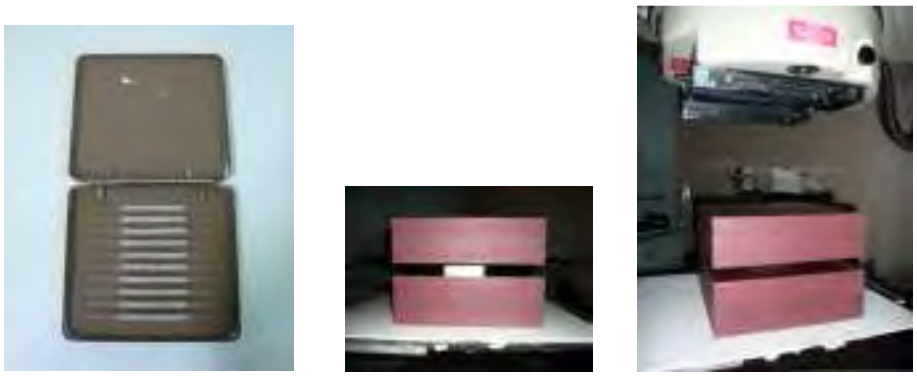

a) b) c)

Fig. 3.17 The TLD sensitivity procedures. a) TLDs in calibration box b) placed TLD expose box between the virtual water slab phantoms c) Irradiated with ^{60}Co

After the TLDs had been exposed, they were removed from the phantom and were read at 24 hr later. The dose were read in the Harshaw model 5500 automatic TLD reader, the unit of TLD reader is shown in Fig.3.18.

Fig. 3.18 The unit of the automatic TLD reader.

B) Linearity

The TLD dosimeters were exposed in body PMMA phantom with 64 slice GE VCT MDCT at department of Radiology, Rajavithi Hospital with 20 mA, 180 mA, 360 mA and 580 mA corresponded to the dose of 1.16 mGy, 10.07mGy, 20.92 mGy and 30.86 mGy, respectively to determine the linearity of the TLD reading.

C) Calibration of TLD

The calibration of TLD was performed by exposing CT x-ray beam with the technique of 120 kV, 100 mA, and 1 sec. The TLDs were stacked in the foam in the z direction of about 10 cm long and placed at the isocenter, the known CTDI measured by 100 mm long pencil ionization chamber at the same position to the TLD was given to the TLDs. The responses of TLDs were equal to the dose given; the radiation correction factor (RCF) in term of nano coulomb per milligray was calculated. The TLD calibration process is shown in Fig.3.19.

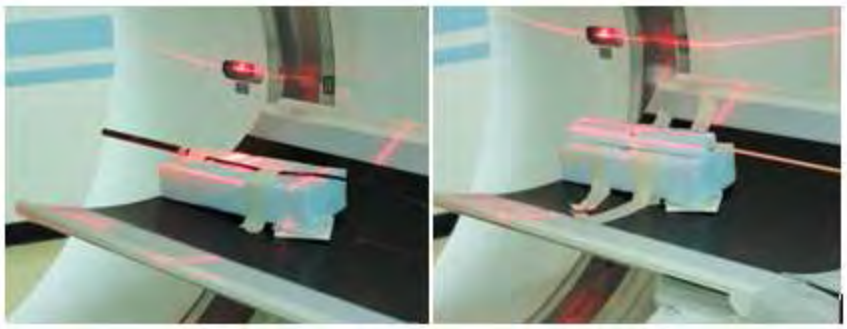

a) b)

Fig. 3.19 The TLD calibrated with CT beam. a) The pencil ionization chamber in air at isocenter. b) The stacked TLDs in the foam at the same position.

The TLD positions in Alderson Rando phantom

Three pieces of TLD chips were loaded into the plastic tubes and placed in each organ of Alderson Rando phantom. The TLDs were positioned with guidance from a human anatomy CT atlas. The exposures were given using routine protocol of brain, chest and abdomen examination. The organ doses were obtained by TLD reading. The effective dose could be estimated from organ dose measurement. They are shown in Fig. 3.20.

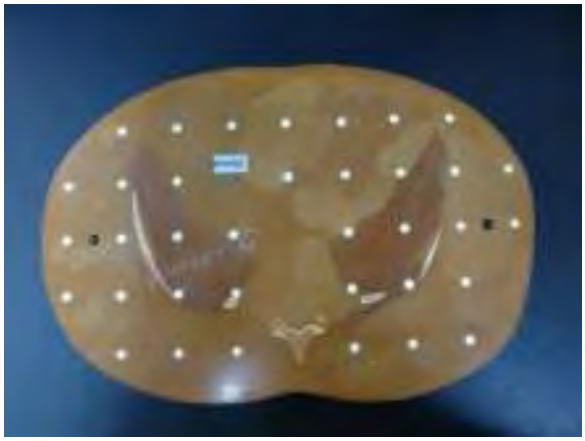

Figure 3.20 The marked position of some organs in a single slice of the phantom.

The Alderson Rando phantom scanning

The Rando phantom with the TLD inserted was scanned in brain, chest and abdominal protocols, which is shown in Fig. 3.21. The exposure parameters are listed in Table 3.2.

Figure 3.21 The Alderson Rando phantom scanning.

The organ and effective dose calculation from TLD in Alderson Rando phantom

The reading values were reported to organ absorbed dose by correcting with the radiation correction factor (RCF) according to equation 2.14. Finally, the organ absorbed doses were converted to the effective dose.

3.8.2 Part 2: The organ and effective doses calculation in patient

3.8.2.1 Monte Carlo simulation method in patient

The details of exposure were kV, average mA, rotation time, pitch and collimation. The patient data were scan region and scan length. All the parameters of each patient were put into the ImPACT spreadsheet for organ and effective doses calculation.

The routine scanning in three examinations are shown in Fig. 3.22 to 3.24.

The brain scan started from base of skull to end of vertex. The scanning range is shown in Fig.3.22. The exposures technique were 120 kV, 200 mA, 0.7 sec, 0.531 pitch, 20 mm collimation, 5mm slice thickness, helical scan, and small head FOV.

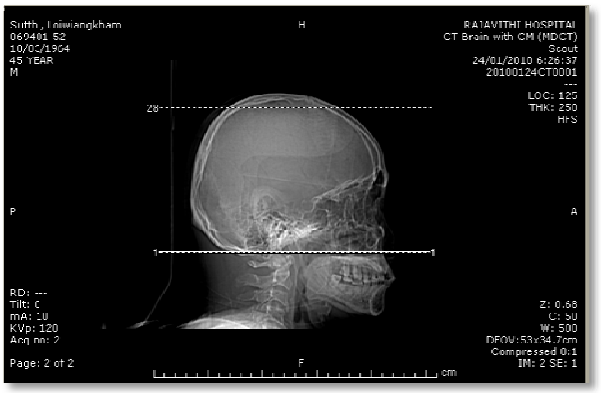

Fig. 3.22 The scan length of routine brain CT scanning.

The chest scan started from apex of lung to end of first lumbar spine (cover of adrenal gland). The scanning range is shown in Fig. 3.23. The exposures technique were 120 kV, Smart mA, 0.6 sec, 1.375 pitch, 40 mm collimation, 5mm slice thickness, helical scan, and medium body FOV.

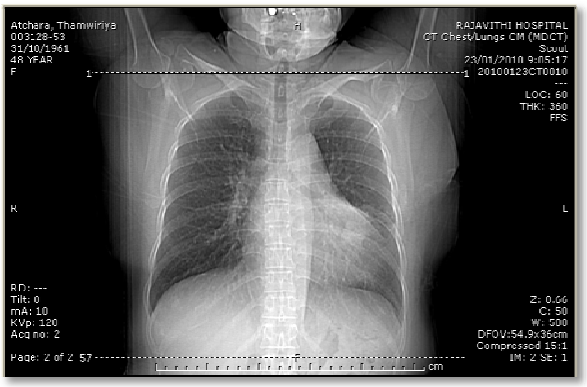

Fig. 3.23 The scan length of routine chest CT scanning.

The whole abdomen scan started from dome of diaphragm to end of pubic symphysis. The scanning range is shown in Fig. 3.24. The exposures technique were 120 kV, Smart mA, 0.6 sec, 0.984 pitch, 40 mm collimation, 5mm slice thickness, helical scan, and medium body FOV.

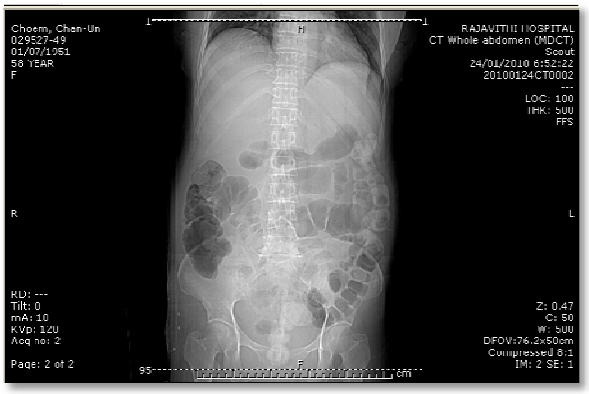

Fig. 3.24 The scan length of routine whole abdomen CT scanning.

3.9 Data collection

The ionization chamber measured the CTDI in air and in the PMMA phantom for Monte Carlo method. The TLDs have been irradiated and they were read out on the Harshaw model 5500 automatic TLD reader for TL dosimetry method. The collection of patients data were put into case record form such as code of patient, gender, age, part of examination, kV, mA, pitch, rotation time, collimation, slice thickness and scan length.

3.10 Data analysis

3.10.1 Summarization of data

The organ and effective doses from CT examination were calculated by ImPACT spreadsheet program for Monte Carlo method and by equation 2.7 for TL dosimetry method. Finally, they were compared for the percentage difference.

3.10.2 Data presentation

The table, bar and scatter graph were presented.

3.11 Benefit of the study

The estimated organ and effective dose for patient underwent computed tomography examinations for 64-slice GE VCT MDCT in department of radiology at Rajavithi Hospital are obtained. The fatal cancer risk of the patient exposed to the radiation could be determined.

3.12 Ethic consideration

Although the measurement was performed in the Alderson Rando phantom and the data of beam and patient parameters were collected from work stations, the ethical were approved by Ethics Committee of Faculty of Medicine, Chulalongkorn University and Rajavithi Hospital.

CHAPTER IV

RESULTS

4.1 Monte Carlo simulation by measurement in Alderson Rando phantom

4.1.1 Measurement of computed tomography dose index

The dose measurement of CTDI in air, head and body PMMA phantom, are shown in Table 4.1. The CTDI measured in air indicated 31.55 mGy for head, 31.61 mGy for body and the mean CTDI measured in head and body phantom indicated 19.72 mGy, 6.24 mGy at the center and 20.09 mGy, 13.64 mGy at the periphery in head and body, respectively. The $CTDI_w$ was calculated for both phantoms, they were 19.97 mGy for head phantom and 11.17 mGy for body phantom.

Table 4.1 The CTDI measurement values in the air, head and body PMMA phantom at 120 kVp, 100 mAs and 10 mm slice thickness.

CTDI measurement	Protocol (mGy/100 mAs)		PMMA phantom (mGy/100 mAs)	
	Head	Body	Head	Body
In air	31.55	31.61		
Center			19.72	6.24
Periphery			20.09	13.64
CTDIw*			19.97	11.17

CTDIw*= the computed tomography dose index weight calculated from $1/3CTDI_{center} + 2/3CTDI_{periphery}$

4.1.2 The organ equivalent doses and effective doses from Monte Carlo simulation in Alderson Rando phantom

The organ equivalent doses together with the tissue weighting factors and the effective doses calculated by ImPACT program of Monte Carlo simulation in head, chest and abdomen protocol in Alderson Rando phantom are summarized in Table 4.2 –Table 4.4, respectively. The exposure technique was the same as routine examination. The high organ equivalent doses in irradiated field showed 37 mSv for brain and 43 mSv for eye lenses in brain examination, the dose ranged from 13 to 19 mSv occurred in lung, stomach, breast, liver, esophagus, adrenal gland, kidney, pancreas, thymus and heart in chest examination and the dose ranged from 16 to 22 mSv found in colon, stomach, bladder, liver, adrenal gland, small intestine, kidney, pancreas and spleen in whole abdomen examination.

The calculated effective doses were 0.9, 9.2, 9.9 mSv in brain, chest and whole abdomen examination, respectively.

Table 4.2 The calculated organ equivalent doses and the effective doses by ImPACT program for brain protocol in Alderson Rando phantom.

Organ	Brain phantom		
	Organ equivalent dose : H_T (mSv)	Tissue weighting factor : W_T	Weighted organ dose (mSv)
Gonads	0.000	0.08	0.000
Bone marrow	2.500	0.12	0.300
Colon	0.000	0.12	0.000
Lung	0.083	0.12	0.010
Stomach	0.003	0.12	0.000
Bladder	0.000	0.04	0.000
Breast	0.025	0.12	0.003
Liver	0.005	0.04	0.000
Esophagus	0.060	0.04	0.002
Thyroid	1.700	0.04	0.068
Skin	2.800	0.01	0.028
Bone surface	11.000	0.01	0.110
Brain	37.000	0.01	0.370
Adrenal gland	0.0016	0.016	0.000
Small intestine	0.00016	0.016	0.000
Kidney	0.0016	0.016	0.000
Pancreas	0.0031	0.016	0.000
Spleen	0.0037	0.016	0.000
Thymus	0.060	0.016	0.001
Muscle	0.940	0.016	0.015
Heart	0.040	0.016	0.001
Effective Dose (mSv)			**0.9**

(Exposures technique: 120 kV, 140 mAs, 0.531 pitch, 20 mm collimation, 5mm slice thickness, helical scan, small head FOV and 14.5 cm scan length)

Table 4.3 The calculated organ equivalent doses and the effective doses by ImPACT program for chest protocol in Alderson Rando phantom.

Organ	Chest phantom		
	Organ equivalent dose: H_T (mSv)	Tissue weighting factor: W_T	Weighted organ dose (mSv)
Gonads	0.150	0.08	0.012
Bone marrow	5.700	0.12	0.684
Colon	1.200	0.12	0.144
Lung	17.000	0.12	2.040
Stomach	13.000	0.12	1.560
Bladder	0.075	0.04	0.003
Breast	14.000	0.12	1.680
Liver	14.000	0.04	0.560
Esophagus	19.000	0.04	0.760
Thyroid	3.300	0.04	0.132
Skin	4.800	0.01	0.048
Bone surface	12.000	0.01	0.120
Brain	0.130	0.01	0.001
Adrenal gland	14.000	0.016	0.228
Small intestine	1.400	0.016	0.023
Kidney	14.000	0.016	0.228
Pancreas	13.000	0.016	0.211
Spleen	8.900	0.016	0.145
Thymus	19.000	0.016	0.309
Muscle	4.900	0.016	0.080
Heart	16.000	0.016	0.260
Effective Dose (mSv)			**9.2**

(Exposures technique: 120 kV, 163 mAs, 1.375 pitch, 40 mm collimation, 5mm slice thickness, helical scan, medium body FOV and 41.0 cm scan length)

Table 4.4 The calculated organ equivalent doses and the effective doses by ImPACT program for abdomen protocol in Alderson Rando phantom.

Organ	Abdomen phantom		
	Organ equivalent dose: H_T (mSv)	Tissue weighting factor: W_T	Weighted organ dose (mSv)
Gonads	8.900	0.08	0.712
Bone marrow	7.400	0.12	0.888
Colon	16.000	0.12	1.920
Lung	4.900	0.12	0.588
Stomach	20.000	0.12	2.400
Bladder	16.000	0.04	0.640
Breast	0.930	0.12	0.112
Liver	18.000	0.04	0.720
Esophagus	0.740	0.04	0.030
Thyroid	0.059	0.04	0.002
Skin	5.800	0.01	0.058
Bone surface	11.000	0.01	0.110
Brain	0.0025	0.01	0.000
Adrenal gland	17.000	0.016	0.276
Small intestine	18.000	0.016	0.293
Kidney	22.000	0.016	0.358
Pancreas	16.000	0.016	0.260
Spleen	18.000	0.016	0.293
Thymus	0.740	0.016	0.012
Muscle	7.400	0.016	0.120
Heart	6.600	0.016	0.107
Effective Dose (mSv)			**9.9**

(Exposures technique: 120 kV, 154 mAs, 0.984 pitch, 40 mm collimation, 5mm slice thickness, helical scan, medium body FOV and 40.0 cm scan length)

4.2 Thermoluminescent dosimeter characteristics

4.2.1. Sensitivity

The sensitivity or the element correction coefficient factors (ECC) of individual TLD chip was sorted by its readout from the same dosage of 5 cGy ^{60}Cobolt gamma radiation. The sensitivity of each TLD was normalized to the average sensitivity to get the sensitivity factors for each TLD according to equation 2.9. The element correction coefficient factors ranged from 0.9003 to 1.0998 (±10%) for the TLD chips that were used in this study. The ECC results of all 102 TLD chips are shown in Table 4.5.

Table 4.5 The sensitivity correction values of 112 TLD chips used for measurement**.**

Number	ECC	Number	ECC	Number	ECC	Number	ECC
1	1.0562	27	0.9173	53	1.0270	79	0.9442
2	0.9333	28	1.0291	54	1.0711	80	0.9211
3	0.9427	29	1.0155	55	1.0650	81	0.9150
4	0.9782	30	1.0050	56	1.0723	82	0.9469
5	0.9491	31	1.0001	57	1.0002	83	0.9257
6	1.0487	32	1.0650	58	0.9710	84	0.9121
7	0.9620	33	1.0313	59	1.0233	85	0.9796
8	0.9869	34	1.0175	60	1.0391	86	0.9596
9	0.9635	35	0.9961	61	0.9846	87	1.0022
10	0.9623	36	0.9003	62	1.0188	88	0.9369
11	0.9705	37	0.9291	63	1.0998	89	0.9054
12	1.0068	38	0.9384	64	1.0307	90	0.9324
13	0.9614	39	0.9103	65	0.9659	91	0.9152
14	1.0105	40	0.9927	66	0.9963	92	1.0341
15	0.9463	41	1.0621	67	1.0162	93	1.0610
16	0.9354	42	0.9898	68	1.0835	94	1.0574
17	0.9676	43	0.9831	69	1.0096	95	0.9809
18	0.9863	44	1.0060	70	1.0315	96	0.9597
19	0.9792	45	1.0648	71	0.9303	97	0.9220
20	1.0294	46	1.0723	72	0.9792	98	0.9404
21	0.9901	47	1.0586	73	0.9327	99	0.9958
22	1.0859	48	0.9832	74	0.9976	100	0.9391
23	1.0432	49	1.0065	75	1.0982	101	1.0840
24	0.9499	50	1.0481	76	1.0052	102	1.0753
25	0.9907	51	1.0321	77	1.0433		
26	0.9954	52	1.0249	78	0.9480	SD	0.09

4.2.2 Linearity

The integral charges corrected by TLD in 10 mm collimated width with the various CTDI values at 1.16 to 30.86 mGy of CT beam measured from the pencil ionization chamber are shown in Table 4.6 and Fig. 4.1. The graph shows the excellent linear relationship between TLDs reading and the absorbed dose responses with the correlation coefficient of 0.999.

Table 4.6 The CTDI in 64 slice GE VCT MDCT and reading value of TLD.

Number	CTDI (mGy)	Dose reading in TLDs (nC)
1	1.16	19.99
2	10.07	172.86
3	20.92	391.71
4	30.86	578.33

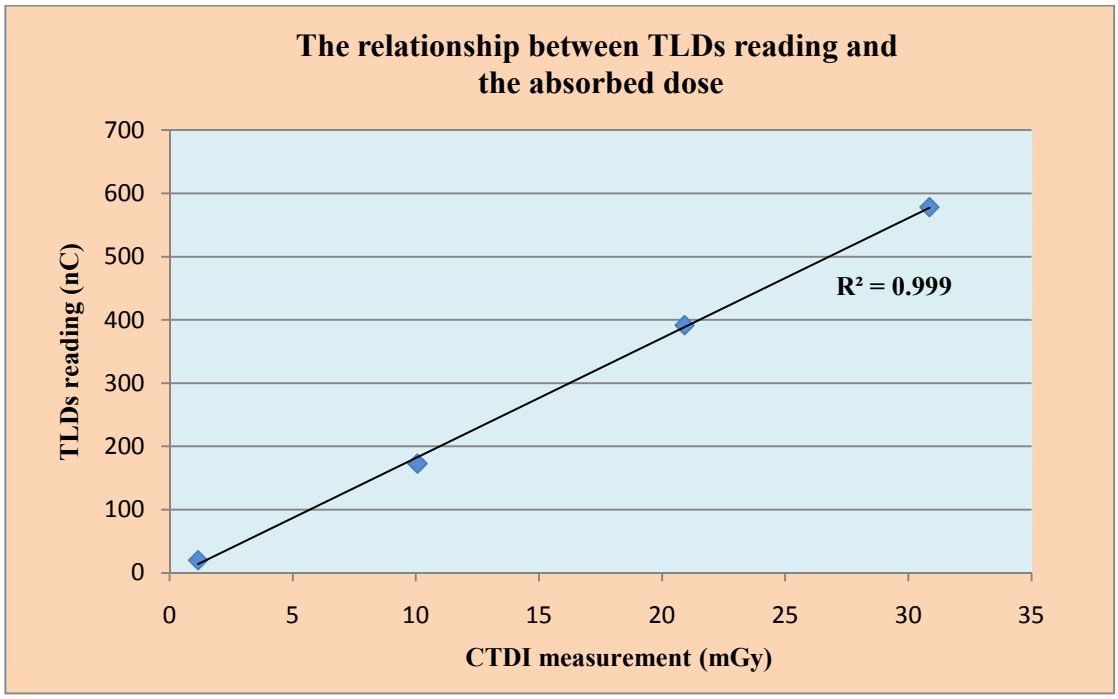

Fig. 4.1 The relation between TLDs response and CTDI

4.2.3 Calibration of thermoluminescent dosimeter

The radiation correction factor of TLD reading was obtained by using the method of the integral value of TLD values in a radiation profile of 10 mm collimated width was equal to the $CTDI_{100}$ dose measured by pencil ionization chamber. The area of under curve was processed by Visual Basic program which was 307.97 nC and the CTDI measurement from MDCT was 28.015 mGy. The radiation correction factor of x-ray beam from CT was 10.993 nC/ mGy.

4.3 The organ equivalent doses and effective doses from TL dosimetry in Alderson Rando phantom

4.3.1 Brain, chest and abdomen protocol

The organ equivalent doses, the tissue weighting factors and the effective doses for TLD measurement of brain, chest and abdomen protocol are summarized in Table 4.7 – Table 4.9. The high organ equivalent doses in irradiated field showed 22.64 mSv for brain and 20.04 mSv for eye lenses in brain examination and the dose ranged from 11.6 to 14.9 mSv occurred in lung, stomach, breast, liver, esophagus, thyroid, adrenal gland, small intestine, kidney, pancreas, spleen, thymus and heart in chest examination, the dose ranged from 11.2 to 18.1 mSv occurred in colon, stomach, bladder, liver, adrenal gland, small intestine, kidney, pancreas, spleen, thymus in whole abdomen examination.

The effective doses were 0.747, 9.336, 9.491 mSv in brain, chest and whole abdomen examination, respectively.

Table 4.7 The measured organ equivalent doses and the effective doses for brain protocol in Alderson Rando phantom.

Organ	Brain phantom		
	Organ equivalent dose: H_T (mSv)	Tissue weighting factor: W_T	Weighted organ dose (mSv)
Gonads	0.005	0.08	0.000
Bone marrow	0.020	0.12	0.002
Colon	0.010	0.12	0.001
Lung	0.051	0.12	0.006
Stomach	0.026	0.12	0.003
Bladder	0.005	0.04	0.000
Breast	0.123	0.12	0.015
Liver	0.032	0.04	0.001
Esophagus	0.059	0.04	0.002
Thyroid	0.815	0.04	0.033
Skin	23.245	0.01	0.232
Bone surface	21.062	0.01	0.211
Brain	22.635	0.01	0.226
Adrenal gland	0.020	0.016	0.000
Small intestine	0.028	0.016	0.000
Kidney	0.011	0.016	0.000
Pancreas	0.025	0.016	0.000
Spleen	0.019	0.016	0.000
Thymus	0.045	0.016	0.001
Muscle	0.776	0.016	0.013
Heart	0.048	0.016	0.001
Effective Dose (mSv)			**0.747**

Table 4.8 The measured organ equivalent doses and the effective doses for chest protocol in Alderson Rando phantom.

Organ	Chest phantom		
	Organ equivalent dose: H_T (mSv)	Tissue weighting factor: W_T	Weighted organ dose (mSv)
Gonads	0.072	0.08	0.006
Bone marrow	11.563	0.12	1.388
Colon	1.240	0.12	0.149
Lung	12.145	0.12	1.457
Stomach	12.253	0.12	1.470
Bladder	0.852	0.04	0.034
Breast	11.617	0.12	1.394
Liver	14.859	0.04	0.594
Esophagus	13.851	0.04	0.554
Thyroid	12.385	0.04	0.495
Skin	7.610	0.01	0.076
Bone surface	0.213	0.01	0.002
Brain	0.181	0.01	0.002
Adrenal gland	12.176	0.016	0.198
Small intestine	13.460	0.016	0.219
Kidney	14.349	0.016	0.233
Pancreas	14.188	0.016	0.231
Spleen	13.359	0.016	0.217
Thymus	14.353	0.016	0.233
Muscle	10.668	0.016	0.173
Heart	13.006	0.016	0.211
Effective Dose (mSv)			**9.336**

Table 4.9 The measured organ equivalent doses and the effective doses for abdomen protocol in Alderson Rando phantom.

Organ	Abdomen phantom		
	Organ equivalent dose: H_T (mSv)	Tissue weighting factor: W_T	Weighted organ dose (mSv)
Gonads	5.543	0.08	0.443
Bone marrow	13.910	0.12	1.669
Colon	11.201	0.12	1.344
Lung	4.423	0.12	0.531
Stomach	15.468	0.12	1.856
Bladder	14.899	0.04	0.596
Breast	1.837	0.12	0.220
Liver	17.212	0.04	0.688
Esophagus	7.662	0.04	0.306
Thyroid	0.203	0.04	0.008
Skin	20.860	0.01	0.209
Bone surface	0.013	0.01	0.000
Brain	0.017	0.01	0.000
Adrenal gland	14.890	0.016	0.242
Small intestine	18.149	0.016	0.295
Kidney	15.114	0.016	0.246
Pancreas	14.730	0.016	0.239
Spleen	16.182	0.016	0.263
Thymus	12.992	0.016	0.211
Muscle	0.214	0.016	0.003
Heart	7.490	0.016	0.122
Effective Dose (mSv)			**9.491**

4.3.2 The Comparison of the organ doses and effective doses between Monte Carlo simulation and TL dosimetry for brain, chest and abdomen protocol.

The calculated organ doses in three examinations which are shown in Table 4.10 illustrated mostly higher dose than the measured, the calculation doses in example were 37, 17 and 20 mGy for brain in brain protocol, lung in chest protocol, and stomach in abdomen protocol, respectively compared to the measurement of 22.64, 12.15 and 15.47 mGy, respectively.

The calculated effective dose in brain, chest and abdomen were 0.9, 9.2 and 9.9 mSv, respectively compared to the measurement of 0.747, 9.336 and 9.491 mSv. The effective doses calculated by ImPACT agreed within 4.3% to those estimated by the TLD measurement for chest and abdomen examination, excepted for brain examination that the difference was 20.5%.

Table 4.10 Comparison of the organ and effective doses between TLD dosimetry and Monte Carlo (MC) simulation for brain, chest and abdomen protocol**.**

Organ	Brain protocol		Chest protocol		Abdomen protocol	
	MC Cal. (mGy)	TLD Meas. (mGy)	MC Cal. (mGy)	TLD Meas. (mGy)	MC Cal. (mGy)	TLD Meas. (mGy)
Gonads	0.000	0.005	0.150	0.072	8.900	5.543
Bone marrow	2.500	0.020	5.700	11.563	7.400	13.910
Colon	0.000	0.010	1.200	1.240	16.000	11.201
Lung	0.083	0.051	17.000	12.145	4.900	4.423
Stomach	0.003	0.026	13.000	12.253	20.000	15.468
Bladder	0.000	0.005	0.075	0.852	16.000	14.899
Breast	0.025	0.123	14.000	11.617	0.930	1.837
Liver	0.005	0.032	14.000	14.859	18.000	17.212
Esophagus	0.060	0.059	19.000	13.851	0.740	7.662
Thyroid	1.700	0.0815	3.300	12.385	0.059	0.203
Skin	2.800	23.245	4.800	7.610	5.800	20.860
Bone surface	11.000	21.062	12.000	0.213	11.000	0.013
Brain	37.000	22.635	0.130	0.181	0.0025	0.017
Adrenal gland	0.0016	0.020	14.000	12.176	17.000	14.890
Small intestine	0.00016	0.028	1.400	13.460	18.000	18.149
Kidney	0.0016	0.011	14.000	14.349	22.000	15.114
Pancreas	0.0031	0.025	13.000	14.188	16.000	14.730
Spleen	0.0037	0.019	8.900	13.359	18.000	16.182
Thymus	0.060	0.045	19.000	14.353	0.740	12.992
Muscle	0.940	0.776	4.900	10.668	7.400	0.214
Heart	0.040	0.048	16.000	13.006	6.600	7.490
ED (mSv)	**0.9**	**0.747**	**9.2**	**9.336**	**9.9**	**9.491**
% ED diff.	**20.5**		**-1.5**		**4.3**	

4.4 The patient data collection

4.4.1 The organ and effective doses in patient calculation

The exposure and patient parameters of brain, chest and abdomen examinations were collected for 180 cases (60 cases in each protocol) of adult male and female patients over 20 years old. The organ and effective doses were calculated using $CTDI_{air}$ and $CTDI_{w}$ from the measurement. The patient data and effective doses calculation result were shown in Table 4.11-Table 4.13 for brain, chest and abdomen, respectively.

Table 4.11 Patient data and exposure parameters of 25 male and 35 female patients for brain examination.

Pt code	Gender	Age (years)	Scan length (cm)	ED (mSv)	Pt code	Gender	Age (years)	Scan length (cm)	ED (mSv)
B01	F	57	13.0	1.5	B31	F	70	14.0	1.6
B02	F	35	13.0	1.5	B32	F	81	13.0	1.5
B03	M	66	13.5	1.6	B33	F	47	13.5	1.6
B04	F	74	13.5	1.6	B34	F	57	13.5	1.6
B05	M	38	14.0	1.6	B35	F	65	13.5	1.6
B06	F	82	13.5	1.6	B36	M	32	14.5	1.7
B07	F	82	13.0	1.5	B37	M	42	12.5	1.5
B08	M	44	14.0	1.6	B38	M	46	13.0	1.5
B09	F	75	13.5	1.6	B39	F	48	12.5	1.5
B10	F	55	13.5	1.6	B40	M	60	12.5	1.5
B11	M	50	13.0	1.5	B41	M	53	13.5	1.6
B12	F	67	12.5	1.5	B42	M	68	14.5	1.7
B13	F	67	12.6	1.5	B43	F	40	13.5	1.6
B14	M	60	13.5	1.6	B44	M	65	14.5	1.7
B15	M	81	13.5	1.6	B45	F	44	13.5	1.6
B16	M	63	13.5	1.6	B46	F	80	13.0	1.5
B17	M	47	12.0	1.4	B47	F	38	13.5	1.6
B18	F	41	12.5	1.5	B48	F	50	12.5	1.5
B19	F	20	14.0	1.6	B49	F	41	12.5	1.5
B20	F	21	14.5	1.7	B50	F	66	12.5	1.5
B21	F	22	14.5	1.7	B51	M	76	13.5	1.6
B22	M	26	14.0	1.6	B52	F	23	13.5	1.6
B23	F	53	12.5	1.5	B53	M	68	14.5	1.7
B24	M	47	14.0	1.6	B54	M	46	13.0	1.5
B25	F	38	13.5	1.6	B55	F	38	13.5	1.6
B26	M	78	14.0	1.6	B56	F	68	13.5	1.6
B27	F	35	13.5	1.6	B57	M	31	14.5	1.7
B28	M	68	14.0	1.6	B58	F	57	13.5	1.6
B29	F	54	12.5	1.5	B59	F	65	13.5	1.6
B30	M	59	13.0	1.5	B60	M	32	14.5	1.7
					Average			**13.4**	**1.6**

B = Brain CT examination,

(Exposures technique: 120 kV, 200 mA (fixed), 0.7 sec., 0.531 pitch, 20 mm collimation, 5mm slice thickness, helical scan, small head FOV, Ref. noise index 3.80 and HVL(head filter) 6.3 mmAl.)

Table 4.12 Patient data and exposure parameters of 26 male and 34 female patients for chest examination.

Pt code	Gender	Age (years)	Scan length (cm)	ED (mSv)	Pt code	Gender	Age (years)	Scan length (cm)	ED (mSv)
C01	F	30	35.0	7.4	C31	F	62	39.0	8.4
C02	F	32	37.0	7.9	C32	F	60	35.0	7.4
C03	F	62	28.5	5.9	C33	M	61	26.5	5.6
C04	M	75	32.5	6.8	C34	F	52	39.9	8.6
C05	M	77	30.0	6.2	C35	M	63	31.5	6.6
C06	F	54	37.5	8.0	C36	F	67	28.5	5.9
C07	M	38	35.5	7.6	C37	F	45	30.6	6.4
C08	M	49	36.0	7.7	C38	M	52	34.2	7.2
C09	F	56	30.8	6.5	C39	M	69	34.0	7.2
C10	F	40	40.0	8.6	C40	F	72	31.5	6.6
C11	F	50	31.0	6.5	C41	M	64	34.0	7.2
C12	M	45	29.5	6.1	C42	F	66	29.0	6.0
C13	M	68	36.5	7.8	C43	F	68	27.0	5.6
C14	F	21	35.0	7.4	C44	F	50	36.0	7.7
C15	F	49	30.9	6.5	C45	F	64	31.4	6.6
C16	M	76	38.5	8.2	C46	F	21	36.0	7.7
C17	F	67	23.1	4.9	C47	M	84	38.5	8.2
C18	F	37	35.5	7.6	C48	F	54	34.0	7.2
C19	M	72	39.5	8.5	C49	M	52	38.0	8.1
C20	F	65	34.0	7.2	C50	F	76	36.0	7.7
C21	M	57	32.0	6.7	C51	F	48	45.3	9.4
C22	M	22	35.0	7.4	C52	M	65	33.5	7.1
C23	F	28	31.0	6.5	C53	M	63	40.0	8.6
C24	M	26	32.5	6.8	C54	M	51	36.5	7.8
C25	F	47	26.0	5.5	C55	F	75	33.0	7.0
C26	F	47	30.5	6.4	C56	F	70	31.3	6.5
C27	M	50	34.0	7.2	C57	F	21	35.0	7.4
C28	M	72	30.0	6.2	C58	M	52	34.2	7.2
C29	F	32	37.0	7.9	C59	F	32	37.0	7.9
C30	M	54	38.0	8.1	C60	M	40	56.6	11.0
					Average			**34.3**	**7.2**

C = Chest CT examination

(Exposures technique: 120 kV, 272 mA (average), 0.6 sec, 1.375 pitch, 40 mm collimation, 5mm slice thickness, helical scan, medium body FOV, Ref. noise index 11.57 and HVL(body filter) 7.5 mmAl.)

Table 4.13 Patient data and exposure parameters of 18 male and 42 female patients for whole abdomen examination.

Pt code	Gender	Age (years)	Scan length (cm)	ED (mSv)	Pt code	Gender	Age (years)	Scan length (cm)	ED (mSv)
A01	F	61	40.5	9.6	A31	F	65	43.0	10.0
A02	F	45	39.5	9.4	A32	F	38	45.5	10.0
A03	F	63	39.0	9.4	A33	F	53	45.0	10.0
A04	F	50	39.0	9.4	A34	F	40	42.5	9.9
A05	F	42	41.0	9.7	A35	F	43	41.5	9.8
A06	M	32	43.0	10.0	A36	F	74	39.0	9.4
A07	F	72	38.5	9.3	A37	F	46	44.0	10.0
A08	M	52	40.0	9.4	A38	M	55	42.0	9.9
A09	F	46	43.5	10.0	A39	F	45	47.0	10.0
A10	M	39	44.5	10.0	A40	F	71	39.5	9.4
A11	M	63	44.5	10.0	A41	M	46	43.0	10.0
A12	F	43	43.0	10.0	A42	F	52	37.0	9.0
A13	M	49	39.5	9.4	A43	F	62	41.5	9.8
A14	M	77	40.5	9.6	A44	F	68	37.0	9.0
A15	F	30	40.5	9.6	A45	F	54	44.0	10.0
A16	M	43	47.5	11.0	A46	M	55	38.0	9.2
A17	F	63	42.5	9.9	A47	M	55	38.0	9.2
A18	M	64	41.1	9.7	A48	F	58	37.0	9.0
A19	F	66	38.0	9.2	A49	F	52	46.0	10.0
A20	F	48	37.0	9.0	A50	F	52	39.0	9.4
A21	F	60	39.0	9.4	A51	F	58	49.5	11.0
A22	F	56	39.5	9.4	A52	F	29	40.0	9.5
A23	F	43	38.0	9.2	A53	F	47	45.5	10.0
A24	F	65	35.0	8.6	A54	M	57	40.5	9.6
A25	M	71	44.5	10.0	A55	M	53	45.0	10.0
A26	F	70	40.0	9.5	A56	M	49	47.5	11.0
A27	F	64	40.0	9.5	A57	F	67	40.5	9.6
A28	F	37	40.0	9.5	A58	F	43	38.0	9.2
A29	M	45	46.0	10.0	A59	M	49	39.5	9.4
A30	F	75	41.5	9.8	A60	F	30	40.5	9.6
					Average			**41.4**	**9.7**

A = Abdomen CT examination

(Exposures technique: 120 kV, 257 mA (average), 0.6 sec, 0.984 pitch, 40 mm collimation, 5mm slice thickness, helical scan, medium body FOV, Ref. noise index 11.57 and HVL(body filter) 7.5 mmAl.)

The summary of the average effective doses and average scan length of patients underwent CT examination is shown in Table 4.14.

Table 4.14 The average mA, average effective doses and average scan length of patients underwent CT examination.

Examination	Average mA	Scan length (cm)		ED (mSv)	
		Aver.	Range	Aver.	Range
Brain	200	13.4 ± 0.65	12.0 – 14.5	1.6 ± 0.07	1.4 – 1.7
Chest	272	34.3 ± 4.99	23.1 – 56.6	7.2 ± 1.03	4.9 – 11.0
Whole Abdomen	257	41.4 ± 3.13	35.0 – 49.5	9.7 ± 0.46	8.6 – 11.0

For brain examination, they were 25 males, 35 females with the average age of 53.4 (20-82) years. The average scan length was 13.4 cm made the average effective dose of 1.6 mSv with the standard deviation of 0.07. The scan length was the main factor for the effective dose as shown in Fig. 4.2. When the scan length increases, the effective dose will increase in linear relationship. The histogram in Fig. 4.3 showed clearly less variation in effective dose value due to small range variation in scan length. The constant of current setting was 200 mA, which was used for the dose calculation.

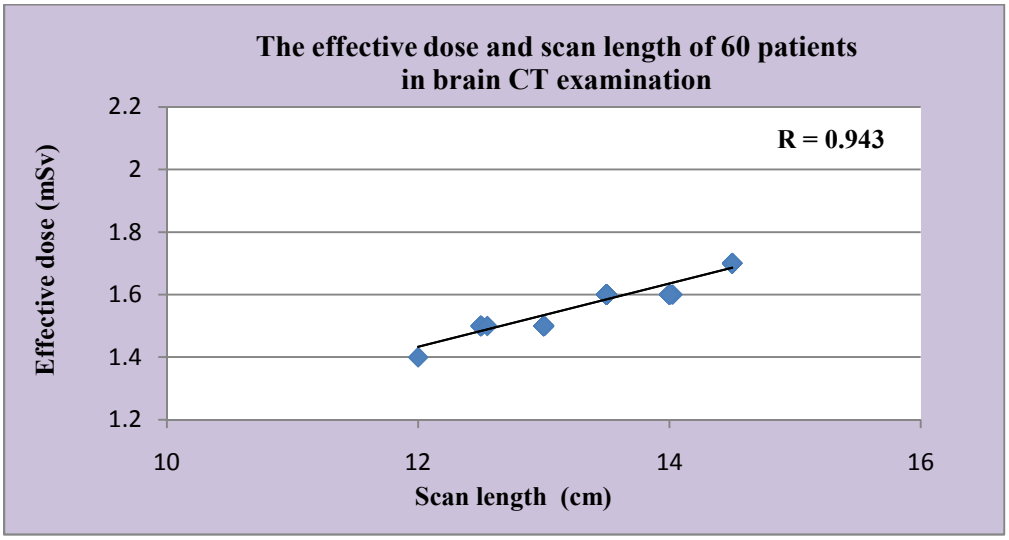

Fig. 4.2 The effective dose and scan length in brain CT examination.

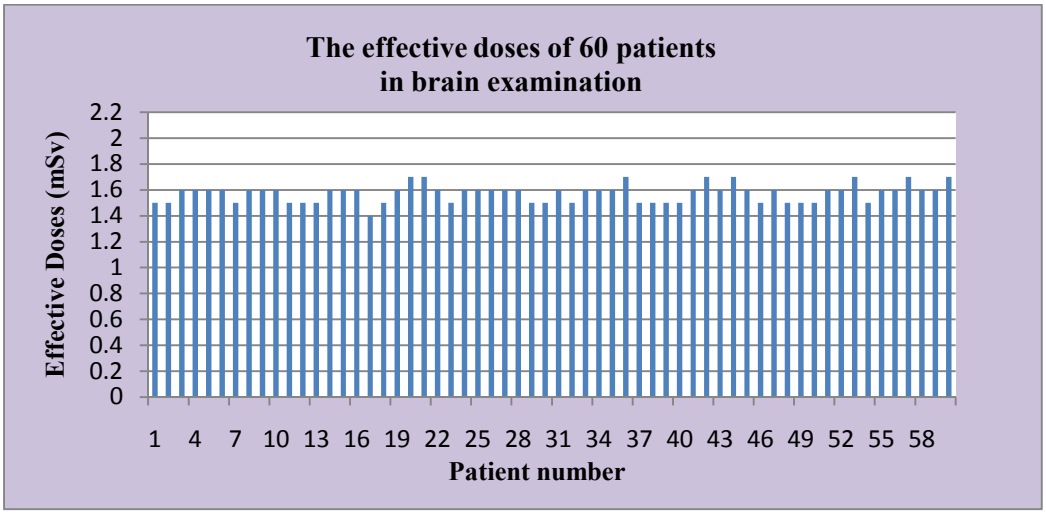

Fig.4.3 The effective doses of patients in brain examination.

For chest examination, they were 26 males, 34 females with the average age of 53.6 (21-84) years. The average scan length was 34.3 cm made the average effective dose of 7.2 mSv with the standard deviation of 1.03. The linear relation between the scan length and the effective dose are shown in Fig. 4.4. The scan length in this examination varied up to 33.5 cm contributed to the more variation in effective dose as shown in histogram of Fig. 4.5. The average current from patient thickness variation was 272 mA, which was used for the dose calculation.

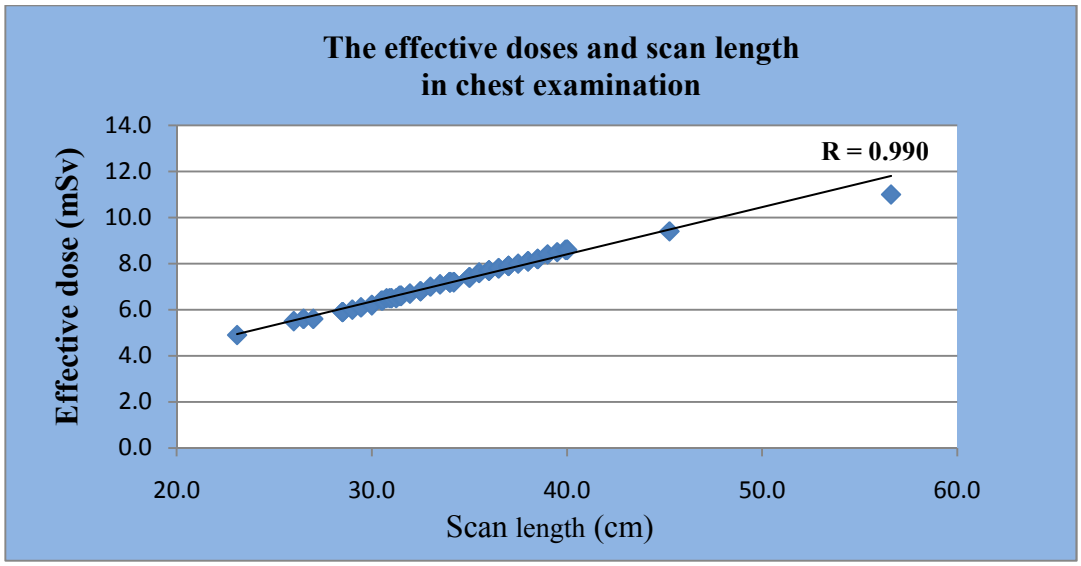

Fig. 4.4 The effective dose and scan length in chest CT examination.

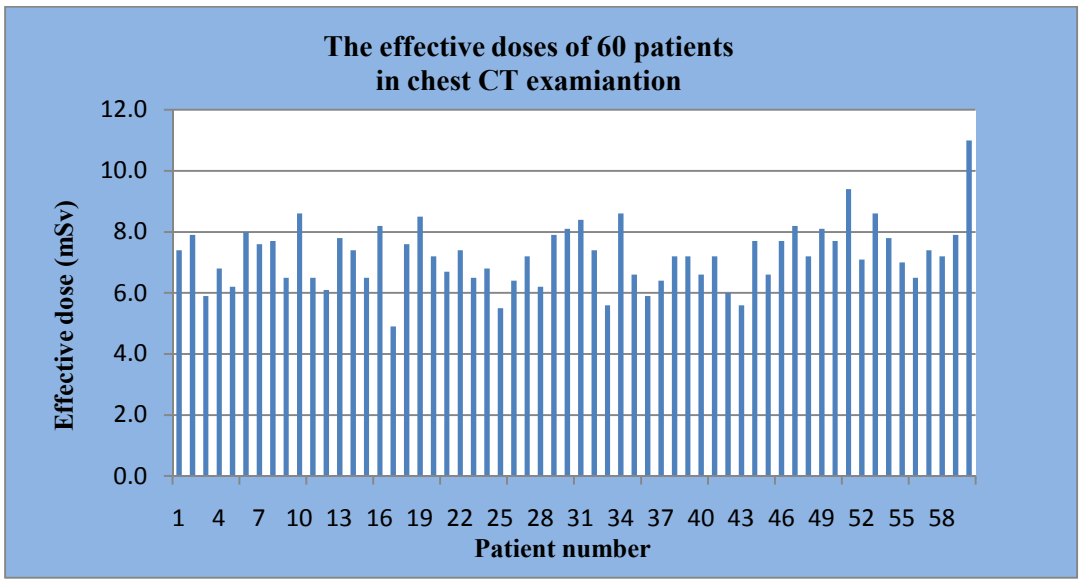

Fig.4.5 The effective doses of patients in chest examination**.**

For whole abdomen examination, they were 18 males, 42 females with the average age of 53.3 (29-77) years. The average scan length was 41.4 cm made the average effective dose of 9.7 mSv with the standard deviation of 0.46. The linear relation between the scan length and the effective dose are shown in Fig. 4.6. However, the last two points shows large deviation this is because of the limitation of program that can show only two digits. So, the long scan length will have large uncertainty. The scan length in this examination varied up to 14.5 cm contributed to the less variation in effective dose as shown in histogram in Fig. 4.7. The average current from patient thickness variation was 257 mA, which was used for the dose calculation.

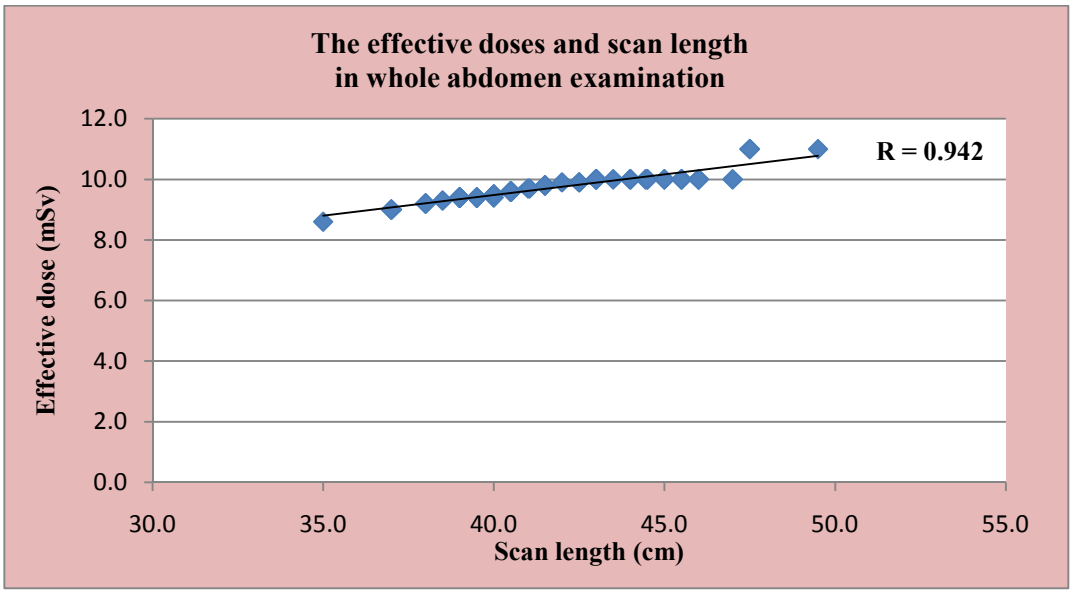

Fig.4.6 The effective dose and scan length in whole abdomen CT examination.

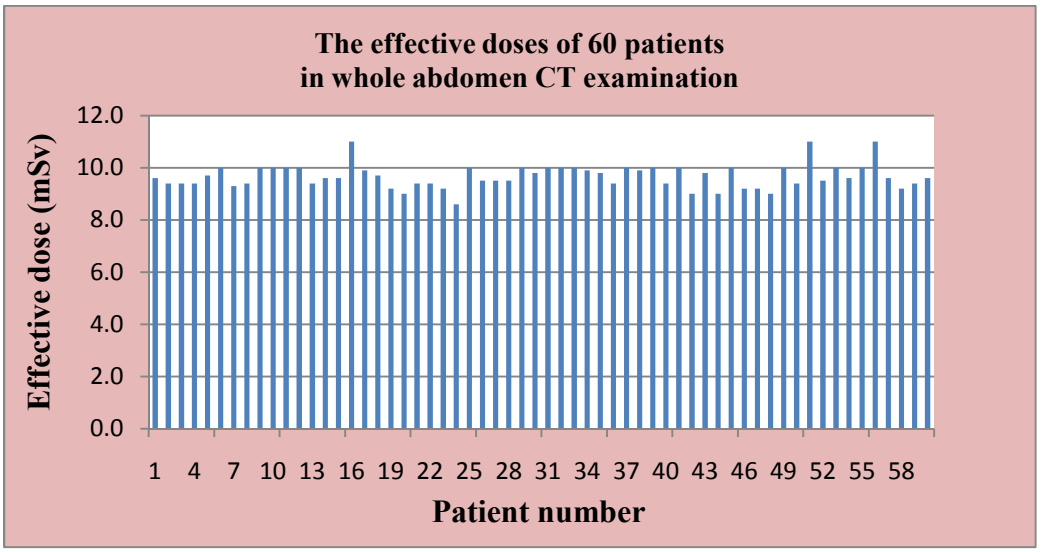

Fig.4.7 The effective doses of patients in whole abdomen examination**.**

The patient organ doses for three examinations in this study compared to the other studies are shown in Table 4.15. The high organ dose in irradiated field showed 37 mGy for brain and 43 mGy for eye lenses in brain examination, the dose ranged from 12 to 19 mGy occurred in lung, breast, esophagus, adrenal gland, thymus and heart in chest examination and the dose ranged from 16 to 22 mGy occurred in colon, stomach, bladder, liver, adrenal gland, small intestine, kidney, pancreas, spleen, ovaries, uterus and prostate for whole abdomen examination.

Table 4.15 The high-irradiated organ doses calculation for brain, chest and whole abdomen examination.

Examination	Organ	Absorbed dose (mGy)
Brain	Brain	37
	Lenses	43
Chest	Lung	17
	Breast	13
	Esophagus	19
	Adrenal gland	12
	Thymus	19
	Heart	16
Whole Abdomen	Colon	16
	Stomach	20
	Bladder	18
	Liver	18
	Adrenal gland	17
	Small intestine	19
	Kidney	22
	Pancreas	16
	Spleen	18
	Ovaries	17
	Uterus/Prostate	18

CHAPTER V

DISCUSSION AND CONCLUSION

5.1 Discussion

5.1.1 Measurement of CTDI

The comparisons of $CTDI_{vol}$ for 100 mAs between measurements, monitor displayed and ImPACT values are shown in Table 5.1.

The $CTDI_{vol}$ of both measurement and monitor values agreed within 9% when compared to the ImPACT in abdomen phantom but they were contrast in head phantom, the $CTDI_{vol}$ values difference went up to 21%. The measured $CTDI_{vol}$ agreed with monitor, so to calculate the organ and effective doses in clinical situation, the monitor $CTDI_{vol}$ could be used for the accuracy within 10%.

Table 5.1 The comparison of $CTDI_{vol}$ (mGy/100 mAs) between measurements, monitor displayed, and ImPACT values.

Protocol	Measurement in PMMA phantom	Monitor	ImPACT	%Diff.* Meas. &ImPACT	% Diff.** Monitor & ImPACT
Head	19.97	20.10	25.30	-21.07	-20.55
Abdomen	11.17	10.11	11.10	0.63	-8.92

*%Difference = ((Measurement – ImPACT)/ ImPACT)*100
**%Difference = ((Monitor – ImPACT)/ ImPACT)*100

5.1.2 Verification of organ and effective dose between calculated and measured

The results demonstrated that most of the calculated organ doses showed higher dose than the TLD dose measurement. The difference has been attributed to design differences between Alderson Rando phantom and MIRD mathematical phantom and also the accurate positioning of TLD of organ dose [18, 19]. The TLD uncertainty of this group has been determined previously [20] with the value of 12%. All these factors contributed to the un-agreement of calculation and measurement in organ dose. The effective dose estimated from TLD dose measurements for chest and abdomen protocol showed a good agreement for 4.3% with the Monte Carlo simulation, the brain showed the difference of 20.5%. The effective doses in brain, chest, and abdomen protocol were comparable with Geleijins study [18] which is shown in Table 5.2.

Table 5.2 The comparison between measurement and calculation study of effective doses (mSv/100mAs) in Alderson Rando phantom of previous study in three examinations.

Studies/ Examination	Scan parameters					Effective dose (mSv/100mAs)		**%Diff. TLD and MC**
	kV	mAs	collimation (mm)	Pitch	Scan length (cm)	TLD meas.	MC cal.	
Brain								
This study	120	140	20	0.531	14.5	0.534	0.643	**20.5**
Geleijins et al.	120	363	10	1.00	12.0	0.52	0.58	**11.54**
Chest								
This study	120	163	40	1.375	41	5.728	5.644	**-1.5**
Geleijins et al.	120	333	10	1.00	27	5.41	4.51	**-16.63**
Abdomen								
This study	120	154	40	0.984	40	6.163	6.429	**4.3**
Geleijins et al.	120	380	10	1.00	30	6.32	5.26	**-16.77**

5.1.3 Estimation of patient dose

For patient examination, the organ and effective doses depended upon the exposure parameters, but the kV, mA, pitch and rotation time were fixed for each examination. So the main variable factor that makes higher organ and effective doses in CT examination is the scan length. The over scanning is another factor that has an effect in increasing patient dose. Sometimes after first scanning, the radiologist ordered more series with the increasing of scan length. The more series of examination is also a factor that increases the organ and effective doses. At least 2 to 4 scan series in CT examinations mostly contributes the more doses from a routine examination CT, however, this study reported CT dose per series. The routine examination at department of Radiology, Rajavithi Hospital for brain, chest and whole abdomen were 1-2 series, 1-3 series and 2-4 series, respectively.

However, for each series of scanning, most of the organ doses were lower than the published work of Heggies J.C.P study [21] which is shown in Table 5.3.

Table 5.3 The comparison of organ absorbed doses with other study.

Examination	Organ	This study Absorbed dose (mGy)	Heggies study Absorbed dose (mGy)
Brain	Brain	37	38
	Lenses	43	45-50
Chest	Lung	17	11
	Breast	13	7
	Esophagus	19	-
	Adrenal gland	12	-
	Thymus	19	-
	Heart	16	-
Whole Abdomen	Colon	16	-
	Stomach	20	30-35*
	Liver	18	
	Kidney	22	
	Bladder	18	-
	Adrenal gland	17	-
	Small intestine	19	22
	Pancreas	16	-
	Spleen	18	-
	Ovaries	17	-
	Uterus/Prostate	18	-

*for stomach, liver and kidney

The effective doses in patient were about 3-25% lower than the ICRP reported, and were about 16-25% higher than Tsapaki V et al study as shown in Table 5.4.

Table 5.4 The comparison of patient effective doses with ICRP reported and other study.

Examination	This study (mSv)	Tsapaki V. et al [14] (mSv)	ICRP [22] (mSv)
Brain	1.6 ± 0.07	1.2	2.0
Chest	7.2 ± 1.03	5.9	8.0
Whole Abdomen	9.7 ± 0.46	8.2	10.0

5.1.4 The effective dose and fatal cancer risk estimation

The average effective doses of three examinations were employed to estimate risk according to ICRP 60, the probability of inducing fatal cancer from a single radiographic exposure is 5 x 10^{-5} mSv^{-1} [23]. The results are shown in Table 5.5.

Table 5.5 Comparison typical effective doses and fatal cancer risks.

Examination	ED (mSv)	Risk 5 x 10^{-5} mSv^{-1}
Brain	1.6	0.8 x 10^{-4}
Chest	7.2	3.6 x 10^{-4}
Whole abdomen	9.7	4.9 x 10^{-4}

The estimated radiation risks are about 1, 4 and 5 cases for 10,000 populations in brain, chest and whole abdomen examination, respectively.

5.2 Conclusion

The verification of ImPACT Calculation Program with TLD in Alderson Rando phantom for brain, chest and abdomen protocols demonstrated the good agreement within 20.5%. The ImPACT Patient Dosimetry Calculction Program version 1.0 can be used for CT dose estimation of the patient. In addition, the use of a computer program is quickly and easily calculated dose. It is extremely useful tool for assessing the effect of changing parameters within the scanning protocol.

The organ doses collected in the patients delivered high doses in irradiated area have the maximum doses of 37 mGy in brain, 19 mGy in esophagus and 22 mGy in kidney for brain, chest and whole abdomen examination, respectively. The effective doses were 1.6 mSv, 7.2 mSv and 9.7 mSv, for brain, chest and whole abdomen examinations, respectively. The risk estimated from this effective dose was still low but careful using CT should be considered.

5.3 Recommendation

The scan length for each patient should be selected individually, based on the scan projection radiograph that is generally made prior to scanning for the purposes of localization, including the number of scan series should be kept as short as necessary. Whenever feasible, critical organ like the eye lenses should be excluded from the scan range.

References

[1] The ImPACT Group. Buyer's guide: Multi-slice CT scanners CEP 08007. Medical Physics Department, Tooting, London (2009).

[2] Tsalafoutas, I. A., and Koukourakis, G. V. Patient dose considerations in computed tomography examination. World Journal Radiology 2 (2010): 262 -268.

[3] International Commission on Radiological Protection. The 2007 Recommendations of the International Commission on Radiological Protection. Publication 103. Ann. ICRP (2007).

[4] Mather, R. The Physics of CT dose. Toshiba Cooperation 2007: www.medical.toshiba.com.

[5] Lee, C. H., et al. Radiation dose modulation technique in the Multidetector CT Era: From basics to practice. RadioGraphics 28(2008): 1451-1459.

[6] Imaging Performance Assessment of CT (ImPACT) CT patient Dosimetry Calculator, Version 1.0. Created 28/08/2009. Available from: *http://impactscan.org/ctdosimetry.htm*

[7] Cameron, J.R., Suntharalingam, N., and Kenney, G.N. Thermoluminescent dosimetry. Milwaukee. The University of Wisconsin Press, 1968.

[8] Izewska, J., and Rajan, G. Radiation Dosimeters. Radiation Oncology Physics 2005:85-89.

[9] Harshaw Bicron radiation measurement produced. Model 5500 automatic TLD reader user's manual Ohio: Saint-Gobian / Norton industrial ceramics, 1993.

[10] Calzado, A., Sanz, S.R., Melchor, M., and Vano E. A Comparison of Measured and Calculated Organ Doses from CT Examinations. Radiation Protection Dosimetry 57 (1995): 381-385.

[11] Fujii, K., et al. Radiation dose evaluation in 64-slice CT examinations with adult and pediatric anthropomorphic phantoms. The British Journal of Radiology 82(2009): 1010-1018.

[12] Lo, G. G., Chan, J. K. F., Lau, C. W., Geng, H., and Yu, S. K. Radiation Dose Survey: Comparison between New-generation Computed Tomography and 64-slice Multidetector Computed Tomography. JHK Coll Radiol 12(2010): 107-112.

[13] Ngaile, J. E., and Msaki, P. K**.** Estimation of patient organ doses from CT examinations in Tanzania. Journal of Applied Clinical Medical Physics 7(2006): 80-94.

[14] Tsapaki, V., et al. Dose Reduction in CT while Maintaining Diagnostic Confidence: Diagnostic Reference Levels at Routine Head, Chest, and Abdominal CT—IAEA-coordinated Research Project. Radiology 240(2006): 828-834.

[15] Brenner, D.J., and Hall, E.J. Computed Tomography An Increasing Source of Radiation Exposure .The New England Journal Medicine 357(2007): 2277-2284.

[16] International Commission on Radiation Units and Measurements. Tissue substitutes in radiation dosimetry and measurement. Report No.44.Bethesda, MD: International Commission on Radiation Units and Measurements (1989).

[17] Shrimpton PC. Electron density values of various human tissues: in vitro Compton scatters measurements and calculated ranges. Phys Med Biol 26(1981): 907.

[18] Geleijins,J., Van , U.J.G., Zoetelief,J., Zweers, D., Broerse, J.J. Comparison of two methods for assessing patient dose from computed tomography. Br J Radiol 67(1994): 360-365.

[19] Hashemi, M.B., and Williams, J.R. A practical approach for the assessment of patient doses from CT examinations. Western General Hospital Edinburgh (2003) Available from*:* www.dundee.ac.uk /medphys/documents/ hashemi.pdf.

[20] Nerysungnoen B. Comparison of effective dose in phantom from computed tomography using Monte Carlo simulation and Thermoluminescent dosimetry methods. The Degree of Master of Science Program in Medidcal Imaging Departmenr of Radiology Faculty of medicine Chulalongkorn University, (2007).

[21] Heggie, J.C.P. (Consultant Medical Physicist BreastScreen). Multi-detector CT (MDCT) Technology&Optimization (Microsoft Powerpoint): RANZCR QUDI Coolum (2009).

[22] International Commission on Radiological Protection, Managing Patient Dose in Computed Tomography. ICRP Publication 87. Annals of the ICRP 30(4) Pergamon Press, Oxford. ; available at www.icrp.org

[23] International Commission on Radiological Protection 60. Recommendations of the International Commission of Radiological Protection. Oxford, UK: Pergamon Press (1991).

Appendices

Appendix A: Case record form

Table 1 Clinical data collection for brain, chest and abdomen in 64 slices GE VCT MDCT examination.

Pt. code	Gender	Age	kV	mA	Pitch (mm/rotation)	Rotation time (sec)	Collimation (mm)	Slice Thickness (mm)	Scan Length (cm)

Appendix B: Quality control of CT system

QC phantom: Water commercial phantom

Serial number: 1003249

Made in U.S.A.

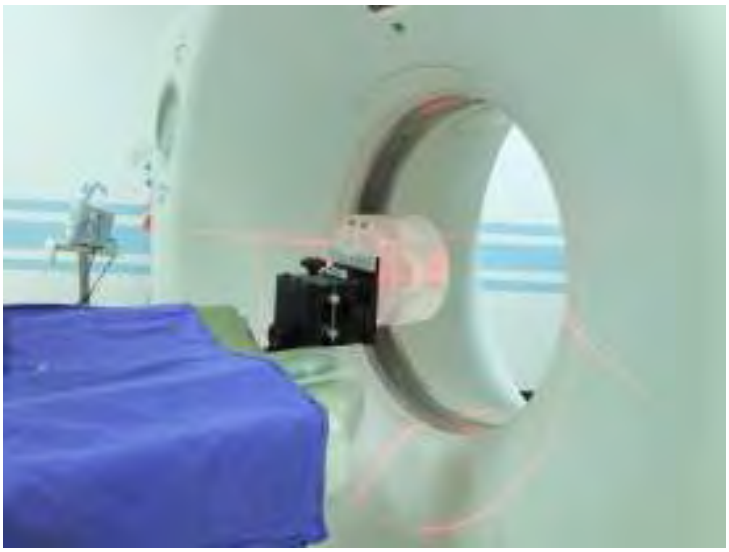

Fig.1 QC phantom alignment.

Report of Quality control CT

25.6º	**Temperature**
48%	**Humidity**
Pass	**Contrast scale**
Pass	**High contrast resolution**
Pass	**Low contrast detestability**
Pass	**Noise and uniformity**
Pass	**Slice thickness test**

This phantom measures six aspects of image quality.

- Contrast scale
- High contrast spatial resolution
- Low contrast detectability
- Noise and uniformity
- Slice thickness
- Laser light accuracy

The QC phantom contains two sections, each corresponding to a single scan plane.

- **Section 1:** Resolution block S0 mm scan location
  - High contrast resolution
  - Contrast scale
  - Slice thickness
  - Laser accuracy
- **Section 2:** Water section is between S40 - S80 mm scan location
  - Noise and uniformity
  - Low contrast detectability

Position the QC Phantom

Place the QC phantom on the phantom holder, and level it. Turn the knob facing the cradle to tilt the top of the phantom away from the gantry. Use the laser alignment lights to position the phantom:

1. Align the axial light to the circumferential line marking section 1.

2. Align the coronal light to the horizontal lines on either side of the phantom.

3. Align the sagittal light (where it strikes the top of the phantom) to the vertical line on the top of the phantom.

4. Position the phantom and select.

Table 2 Parameters for QC.

Interface	**Input**	
Entry	Head First	
Position	Supine	
Anatomical reference	QC	
Scan range	I =0, S = 80	
Thickness	5 , 40 mm aperture	
Reconstruction Interval	5	
Tilt Tube	0 degree	
Scan FOV	Small body	
kV	120	
mA	335	
Rotation Speed	0.4 seconds	Pitch 0.516
Scan Range	Prescribe 1 scan group with 3 reconstruction	
Group 1	**Algorithm, DFOV**	**Test**
Reconstruction 1	Standard, 25 cm DFOV	High contrast resolution, Low contrast detectability, Noise and uniformity
Reconstruction 2	Bone, 15.0 cm DFOV	High contrast resolution
Reconstruction 3	Standard, 22.7 cm DFOV	Low contrast detectability
Matrix	512	
Contrast	None	
Special processing	None	

Perform the following:

a) Contrast scale test at scan location S0 of the helical scan.

b) High contrast spatial resolution test at scan location S0 of the helical scan.

c) Low contrast detectability test at scan location S40 - S80 of the helical scan.

d) Noise and uniformity test at scan location S40 - S80 of the helical scan.

e) Slice thickness test at scan location S0 of the axial slice thickness scans.

f) Alignment light accuracy test at scan location S0 of the alignment light test scan.

Contrast scale

Purpose:

The CT values of water and plexiglass in the phantom represent the standard against which you track the system contrast scale over time.

Tolerance: The difference should equal 120 ± 12

a) 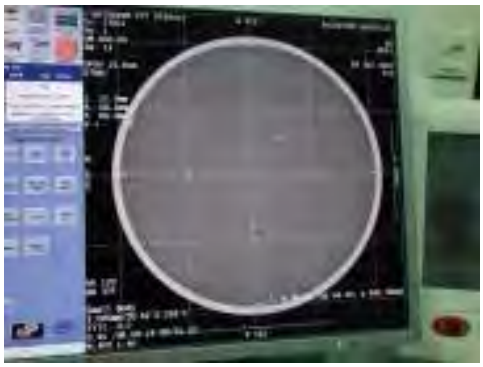 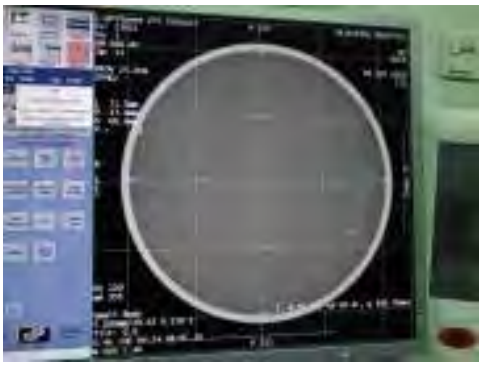 b)

c)  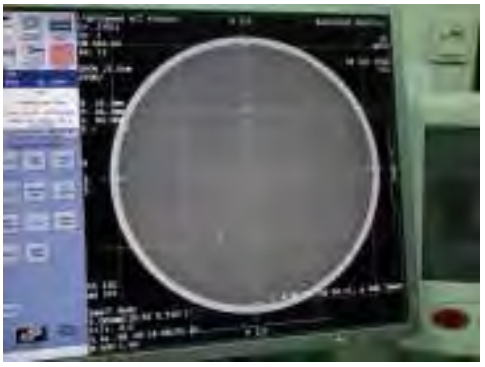 d)

Fig.2 Contrast scale phantom section.

Table 3 Results of Contrast Scale**.**

Position	CT number	SD
a) 12 o'clock (0,8)	1.05	± 4.82
b) 3 o'clock (8,0)	1.10	± 4.74
c) 6 o'clock (0,-8)	1.49	± 4.54
d) 9 o'clock (-8,0)	1.61	± 4.42
Over plexiglass above line pattern (-2,2)	126.29	± 5.04
Over plexiglass below line pattern (2,-2)	126.13	± 5.21

Average CT number of water (1.05+1.10+1.49+1.61)/4 = 1.3125
Average CT number of Plexiglass (126.29+126.13)/2 = 126.21
Subtract the CT number of water from the CT number of plexiglass
(126.21 -1.3125) = **124.89** (**Pass**)

High contrast spatial resolution

Method:

Section 1 of the phantom contains six sets of bar patterns in a plexiglass block used to test high contrast spatial resolution. Each pattern consists of sets of equally sized bars and spaces. Water fills the spaces and provides about 12% (120 HU) contrast. The resolution block contains the following bar sizes: 1.6mm, 1.3mm, 1.0mm, 0.8mm, 0.6mm, and 0.5mm. Position box ROI over the bar pattern, and size it to fit within the bar pattern.

Tolerance: The standard deviation for ROI in the 1.6 bar pattern should equal 37 ± 4

a)  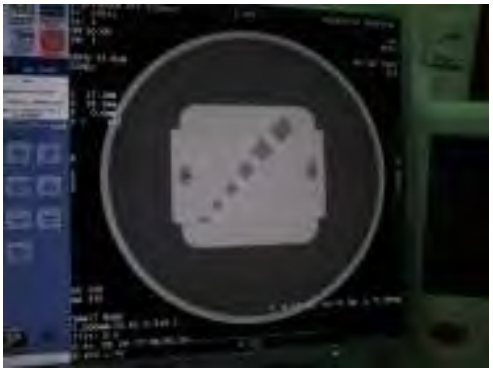 b)

c) 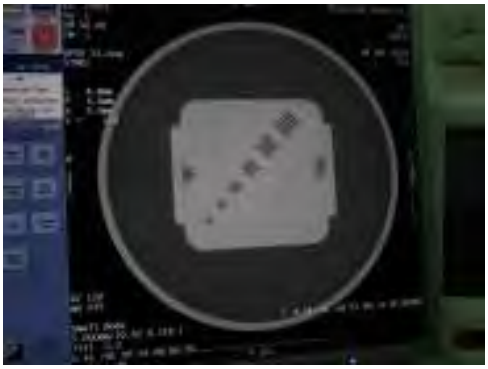  d)

e)   f)

Fig.3 High contrast spatial resolution section.

Table 4 Results of high contrast spatial resolution**.**

Bar size(mm)	CT number	Standard Deviation
a) 1.6	67.36	39.65
b) 1.3	67.14	33.58
c) 1.0	68.28	23.44
d) 0.8	67.29	12.21
e) 0.6	69.00	6.91
f) 0.5	65.50	6.80

The results were 39.65 which it was in range 33 - 41 for the standard algorithm**.** Eye checks about **5 groups**.

Low contrast detectability

Method:

Low contrast detectability (LCD) refers to the visibility of small objects at low contrast levels. In practical terms; it can be defined as the contrast required resolving an object of a given diameter at a given dose. Traditionally, one would image a tissue-equivalent phantom containing small, low-contrast objects, and visually inspect the images. GE recommends a statistical method of quantifying LCD based upon the noise properties of a standard image. Since this method yields a quantitative measurement, as opposed to a visual verification, it is suitable for daily tracking of system image quality. Scan the quality control phantom using the daily image quality protocol. Analyze the images from recon 3, the water section (locations S40 to S80).

Tolerance: accept at ≥ 4 holes

a) 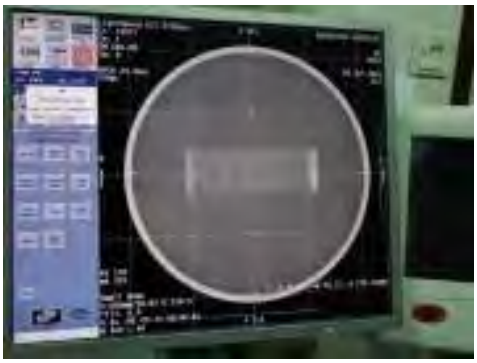  b)

c) 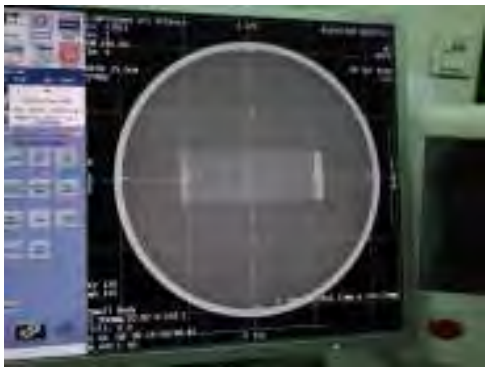  d)

Fig.4 Image analyzes low contrast detectability.

Table 5 Results of low contrast detectability.

Position	CT number	SD
ROI over the polystyrene, just above the holes	16.84	± 4.75
ROI over the water section, just above the membrane	0.05	± 4.41
ROI over the polystyrene, just below the holes	16.48	± 4.46
ROI over the water section, just below the membrane	-0.07	± 4.75

Number of visible holes = see 5 holes

Noise and Uniformity

Method:

Section 3 of the phantom tests noise and uniformity. Use any scan location from S40 - S80 (recon 1). Noise limits low contrast resolution, and masks anatomy with similar structure to surrounding tissue. QC phantom section 2 (recon 1) provides a uniform image by which to assess image CT number noise and uniformity. Use the standard algorithm to reconstruct the image.

Tolerance:

If the image is reconstructed with standard algorithm and small SFOV, the mean of center ROI should equal 0 ± 3.

Standard Deviation of center ROI should equal 3.2 ± 0.3.

The uniformity difference between the center ROI and the average of the edge ROIs should be 0 ± 3.

Table 6 Results of noise and uniformity**.**

Position	CT number	SD (noice)
Center of image (0,0)	0.84	± 3.02
12 o'clock (0,8)	0.88	± 2.62
3 o'clock (8,0)	0.54	± 2.57
6 o'clock (0,-8)	0.60	± 2.87
6 o'clock (-8,0)	0.85	± 2.75

Standard Deviation of center ROI of results equal 3.02 and periphery ROI not exceed 3.

Slice Thickness Test

The resolution block contains holes drilled 1mm apart and positioned to form a line at 45 degrees to the scan plane. Each visible hole in the image represents 1mm of beam thickness.

Table 7 QC Protocol for slice thickness.

Interface		**Input**		
Entry		Head first		
Position		Supine		
Anatomical reference		QC		
Landmark Location		0 on resolution phantom at circumferential line/cross hatch.		
Scan type		Axial		
Scan Range		Prescribe 1 scan group with 3 reconstruction		
Group 1		**Thickness**	**Scan range**	**Spacing**
	Recon 1	5mm/8i	I17.5 - S17.5	0
	Recon 2	2.5mm/16i	I18.75 - S18.75	0
Group 2		**Thickness**	**Scan range**	**Spacing**
	Recon 1	1.25mm/16i	I9.37 - S9.37	0
Tilt Tube		0 degree		
Scan FOV		Small		
kV		120		
mA		260		
Rotation Speed		1 seconds		
DFOV		25 cm		
Algorithm		Standard		
Matrix		512		
Contrast		None		
Special processing		None		

Tolerance: Slice thickness should not vary by more than ± 1 mm from the expected value, when evaluated according to instructions.

Recommended window width: 250

Recommended window level:

- -100 for 1.25mm, -25 for 2.5mm and + 50 for 5.0mm

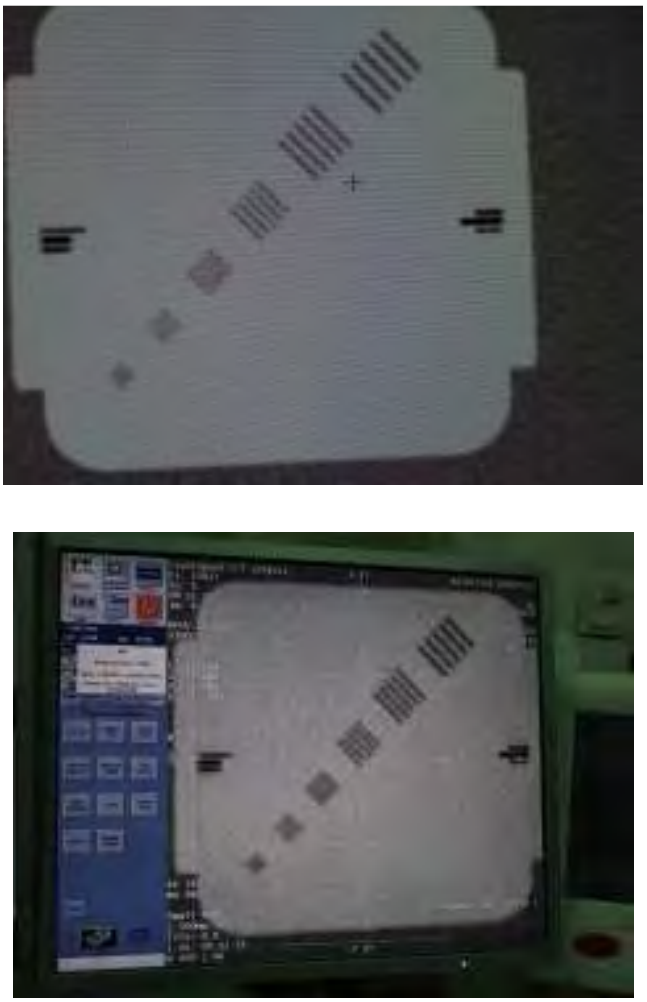

Fig.5 Slice thickness lines.

Table 8 Results of slice thickness test.

Slice thickness(mm)	Window width / Level	Number of visible lines
1.25	250 / -100	1.5
2.50	250 / -25	2.75
5.00	250 / 50	5.5

The results were seeing over 0.25 lines for each of scan thickness.

Vitae

Name Mrs.Ratirat Puekpuang

Date of birth September 25, 1966

Place of birth Nakhonsawan, Thailand

Education Bachelor of Education in Health Education Program
Faculty of Education
Nakhonsawan Teacher's College, 1991

Bachelor of Science in Radiological Technology program
Faculty of Medical technology
Mahidol University, 1997

Work Experiences 1988 – 2000
Radiological Technologist, Department of Radiology
Phayuhakiri Hospital
Nakhonsawan

2000 – Present
Radiological Technologist, Department of Radiology
Sawanpracharak Hospital
Nakhonsawan

Award The 2nd Best Diagnostic Radiology Poster Presentation in the title is "*Organ and Effective Doses from the Multiple Detector Computed Tomography of Chest Examination*" from 8th South-East Asian Congress of Medical Physics (SECOMP), Biophysics, and Biomedical Engineering
Bandung, Indonesia

International Congress

The Japan Congress of Radiology (JRC) and the scientific annual meeting for Japanese Society of Radiological Technology (JSRT) on April 8-10, 2010
Yogohama city, Japan

The 8th South-East Asian Congress of Medical Physics (SECOMP), Biophysics, and Biomedical Engineering on December 11-12, 2010, Bandung, Indonesia

Adress 633/30 Mue 2 Tambol Nongpling Amphor Meang,
Nakhonsawan 60000